Neoplasia • Vol. 7, No. 6, June 2005, pp. 556–562 556

www.neoplasia.com

Array-Based Comparative Genomic Hybridization Identifies Localized DNA Amplifications and Homozygous Deletions in Pancreatic Cancer[1]*

Murali D. Bashyam[*,†], Ryan Bair*[*], Young H. Kim*[*], Pei Wang*[‡], Tina Hernandez-Boussard*[§], Collins A. Karikari*[¶], Robert Tibshirani*[‡,#], Anirban Maitra*[¶] and Jonathan R. Pollack*[*]

[*]Department of Pathology, Stanford University, Stanford, CA, USA; [†]Center for DNA Fingerprinting and Diagnostics, Nacharam, Hyderabad, India; Department of [‡]Statistics; Department of [§]Genetics, Stanford University, Stanford, CA, USA; [¶]Department of Pathology, The Johns Hopkins University, Baltimore, MD, USA; [#]Department of Health Research and Policy, Stanford University, Stanford, CA, USA

Abstract

Pancreatic cancer, the fourth leading cause of cancer death in the United States, is frequently associated with the amplification and deletion of specific oncogenes and tumor-suppressor genes (TSGs), respectively. To identify such novel alterations and to discover the underlying genes, we performed comparative genomic hybridization on a set of 22 human pancreatic cancer cell lines, using cDNA microarrays measuring ~26,000 human genes (thereby providing an average mapping resolution of <60 kb). To define the subset of amplified and deleted genes with correspondingly altered expression, we also profiled mRNA levels in parallel using the same cDNA microarray platform. In total, we identified 14 high-level amplifications (38–4934 kb in size) and 15 homozygous deletions (46–725 kb). We discovered novel localized amplicons, suggesting previously unrecognized candidate oncogenes at 6p21, 7q21 (*SMURF1*, *TRRAP*), 11q22 (*BIRC2*, *BIRC3*), 12p12, 14q24 (*TGFB3*), 17q12, and 19q13. Likewise, we identified novel polymerase chain reaction–validated homozygous deletions indicating new candidate TSGs at 6q25, 8p23, 8p22 (*TUSC3*), 9q33 (*TNC*, *TNFSF15*), 10q22, 10q24 (*CHUK*), 11p15 (*DKK3*), 16q23, 18q23, 21q22 (*PRDM15*, *ANKRD3*), and Xp11. Our findings suggest candidate genes and pathways, which may contribute to the development or progression of pancreatic cancer. *Neoplasia* (2005) **7,** 556–562

Keywords: Pancreatic cancer, array CGH, comparative genomic hybridization, expression profiling, DNA amplification.

Introduction

Pancreatic cancer is the fourth leading cause of cancer death in the United States. With a 5-year survival rate of less than 5%, mortality rates closely mirror incidence rates, reflecting the ineffectiveness of current treatment regimens [1]. An improved understanding of the molecular pathogenesis of pancreatic cancer is urgently needed to identify new targets and strategies for effective therapy [2].

As with other solid tumor types, the amplification of oncogenes and deletion of tumor-suppressor genes (TSGs) play a critical role in the development and progression of pancreatic cancer. Activating mutations—and less frequently amplification [3,4]—of the *KRAS2* oncogene (12p12), for example, have been identified as early events in nearly all pancreatic adenocarcinomas [2]. Likewise, the *CDKN2A*, *TP53*, and *SMAD4* TSGs are frequently deleted or inactivated by mutation or promoter hypermethylation [2]. Indeed, the discovery of homozygous deletions first led to the identification of *CDKN2A* and *SMAD4* as important TSGs [5,6].

Pancreatic cancers likely harbor additional localized DNA amplifications and deletions that are not apparent by conventional cytogenetic techniques such as comparative genomic hybridization (CGH) [7]. Array-based CGH (aCGH) methods provide an alternative higher-resolution approach for identifying these lesions [8–10]. In the current study, we have performed a cDNA microarray-based CGH analysis to identify localized DNA amplifications and deletions in a set of pancreatic cancer cell lines. In parallel, we have measured mRNA levels using the same microarray platform, thereby defining the subset of amplified/deleted genes displaying correspondingly altered expressions.

Materials and Methods

Pancreatic Cancer Cell Lines

AsPC-1, BxPC-3, Capan-1, Capan-2, CFPAC-1, HPAC, HPAF-II, Hs 766T, MIA PaCa-2, MPanc96, PANC-1, Panc

Abbreviations: aCGH, array-based comparative genomic hybridization; FISH, fluorescence *in situ* hybridization; TSG, tumor-suppressor gene

Address all correspondence to: Jonathan R. Pollack, MD, PhD, Department of Pathology, Stanford University School of Medicine, 269 Campus Drive, CCSR 3245A, Stanford, CA 94305-5176. E-mail: pollack1@stanford.edu

[1]This work was supported, in part, by a grant from the Lustgarten Foundation. M.D.B. was also supported by a Biotechnology Overseas Associateship from the Department of Biotechnology, Ministry of Science and Technology, Government of India.

*This article refers to supplementary material which is designated by "W" (ie, Table W1, Figure W1) and is available online at www.bcdecker.com

Received 31 August 2004; Revised 12 October 2004; Accepted 18 October 2004.

DOI 10.1593/neo.04586

02.03, Panc 02.13, Panc 03.27, Panc 08.13, Panc 10.05, PL45, SU.86.86, and SW 1990 were obtained from the American Type Culture Collection (ATCC, Manassas, VA). PL5 and PL8 were obtained from Dr. Anirban Maitra (Johns Hopkins University, Baltimore, MD). Colo-357 was a kind gift of Dr. Caroline Hill (Cancer Research UK London Research Institute, London, UK). Cell lines (Table W1) were grown to 80% confluence in RPMI 1640 medium supplemented with 10% fetal bovine serum. Genomic DNA was isolated using the Qiagen (Valencia, CA) Blood and Cell Culture DNA Maxi Kit, and RNA was isolated using the Trizol (Invitrogen, Carlsbad, CA) method.

Array CGH and Gene Expression Profiling

cDNA microarrays spotted on Corning (Corning, NY) UltraGAPS coated slides were obtained from the Stanford Functional Genomics Facility (Stanford, CA). These arrays contain 39,632 human cDNA, representing approximately 25,856 mapped human genes (22,890 UniGene clusters [11] together with 2966 additional mapped expressed sequence tags not assigned UniGene IDs). aCGH and gene expression profiling were performed essentially as described [12,13]. Briefly, for aCGH, 4 μg of genomic DNA from each cell line was random primer–labeled with Cy5 and cohybridized to the cDNA microarray along with 4 μg of Cy3-labeled sex-matched normal leukocyte reference DNA. For gene expression profiling, 50 μg of total RNA from each cell line and 50 μg of reference RNA (derived from 11 different established human cell lines) were differentially labeled with Cy5 and Cy3, respectively, and cohybridized to cDNA microarrays. Following overnight hybridization and washing, arrays were imaged using a GenePix 4000B scanner (Axon, Union City, CA). Fluorescence ratios were extracted using GenePix Pro 5.0 software, and the data were uploaded into the Stanford Microarray Database [14] for storage, retrieval, and analysis. The complete microarray datasets are available at http://smd.stanford.edu.

Data Analysis

For aCGH, background-subtracted fluorescence ratios were normalized for each array by setting the average fluorescence ratio for all array elements equal to 1. Genes were considered reliably measured if the fluorescence intensity for the Cy3 reference channel was at least 1.4-fold above background. Map positions for arrayed cDNA clones were assigned using the NCBI genome assembly, accessed through the UCSC genome browser (July 2003 freeze). For genes represented by multiple arrayed cDNA, the average fluorescence ratio was used. DNA copy number gains and losses were identified using the CLuster Along Chromosomes (CLAC) method (http://www-stat.stanford.edu/~wp57/CGH-Miner) [15]. Briefly, the CLAC algorithm builds a hierarchical cluster–style tree along each chromosome, such that neighboring genes with positive and negative ratios are separated into different clusters. Gains and losses are then called significant based on the height and width of clusters, and a false discovery rate is estimated by comparison to normal–normal hybridization data. We defined high-level DNA amplifications and presumptive homozygous deletions as contiguous regions identified by CLAC, with at least 50% of genes displaying fluorescence ratios ≥ 3 or ≤ 0.25, respectively. For expression profiling, fluorescence ratios were normalized for each array, and then well-measured genes (fluorescence intensities for the Cy5 or Cy3 channel at least 1.5-fold above background) were subsequently "mean-centered" (i.e., reported for each gene relative to the mean ratio across all samples).

Fluorescence In Situ Hybridization (FISH)

To validate DNA amplification, we performed interphase FISH using a Spectrum Green–labeled bacterial artificial chromosome probe corresponding to the 7q21 locus (RP11-62N3; Children's Hospital Oakland Research Institute, Oakland, CA) and a Spectrum Orange–labeled chromosome 7 centromere probe (CEP 7; Vysis, Downers Grove, IL). FISH was performed exactly according to the Vysis labeling and hybridization protocols, and images were captured using an Olympus (Melville, NY) BX51 microscope and CytoVision 3.0 software (Applied Imaging Corp., San Jose, CA).

Polymerase Chain Reaction (PCR) Validation of Homozygous Deletions

To validate homozygous deletions, we used gene-specific primer pairs to PCR-amplify genomic DNA from cell lines. Primer pairs for genes flanking the regions of homozygous deletion, and designed to have a distinguishable fragment size, were included in the PCR reactions as internal controls. PCR was performed on an Applied Biosystems (Foster City, CA) GeneAmp 9700, using 100 ng of DNA template, 1× PCR buffer (Applied Biosystems), 160 μM dNTPs, 1.5 mM MgCl, 10 pmol of each individual primer (Table W2), and 1 U of Taq DNA polymerase (Applied Biosystems) in a 25-μl reaction for 35 cycles [94°C, 30 seconds; annealing temperature (Table W2), 30 seconds; 72°C, 30 seconds], followed by gel electrophoresis on a 1.8% TAE agarose gel, and visualization using an Alpha Innotech (San Leandro, CA) imaging system.

Results

To identify DNA amplifications and deletions, we performed CGH on a set of 22 pancreatic adenocarcinoma cell lines using cDNA microarrays measuring 25,856 human genes, thereby providing an average mapping resolution of less than 60 kb. We identified numerous chromosomal regions of recurrent gain and loss (Figures W1 and W2), the spectrum of which was consistent with published conventional CGH studies [4,16–20]. Gains were most commonly observed on chromosomes 8q (90%), 11q (75%), 20q (75%), 7q (65%), 3q (60%), 5q (60%), and 7p (60%), whereas losses occurred most often on 18q (95%), 8p (80%), 4q (70%), 6q (65%), 9p (65%), 17p (65%), 3p (60%), 6p (60%), and Xp (60%). Cell lines PL45 and Panc 10.05 displayed highly similar aCGH profiles, consistent with their being established from the same patient. Surprisingly, cell lines AsPC-1 and MPanc96, the latter obtained both from the ATCC repository and from the originator [21], also exhibited

Table 1. High-Level DNA Amplifications Identified by aCGH.

Cytoband	P Border (nt)	Q Border (nt)	Size (kb)	Cell Line	Remaining Lines with Low-Level Gain	Selected Candidate Oncogenes*
6p21	32,043,837	32,410,885	367	SW 1990	4/19	STK19, TNXB, **PBX2**, NOTCH4
6p21	32,827,514	32,865,810	38	SW 1990	0/19	**TAP1**
7q21	93,671,907	98,605,497	4934	AsPC-1	9/19	**TRRAP**, **SMURF1**, **ARPC1A**, **ARPC1B**
11q13	69,241,850	70,008,988	767	Colo-357	14/19	**CCND1**, EMS1
11q22	101,406,590	102,133,375	727	Colo-357	4/19	**YAP1**, **BIRC2**, **BIRC3**, MMP7, MMP27
12p12	14,926,093	15,186,368	260	Su.86.86	4/19	
12p12	25,253,402	26,380,345	1127	Su.86.86	5/19	**KRAS2**
12p11	25,253,402	27,366,920	2114	HPAF-II	5/19	**KRAS2**, **FGHR1OP2**, **STK38L**
14q24	74,414,776	74,540,126	125	Panc 08.13	6/19	TGFB3
17q12	36,065,530	36,106,569	41	CFPAC-1	5/19	
19q13	39,957,195	40,808,091	851	Su.86.86	8/19	USF2
19q13	43,616,179	45,546,133	1930	PANC-1	7/19	**eIF3k**, AKT2
19q13	43,997,907	46,073,560	2076	Su.86.86	7/19	AKT2
19q13	55,171,535	55,539,817	368	Su.86.86	6/19	**ZNF473**

*Boldface type indicates that gene expression was well measured by microarray analysis and elevated when amplified.

nearly identical profiles. Given that AsPC-1 was established 15 years earlier [22], we conclude that both cell lines likely represent AsPC-1.

In addition to these broad regions of chromosomal gain and loss, we also identified numerous localized high-level DNA amplifications (i.e., fluorescence ratios $\geq$3, corresponding to at least five-fold amplification [9]; Table 1) and presumptive homozygous deletions (i.e., fluorescence ratios $\leq$0.25; Table 2). All together, we identified 14 high-level amplifications in eight different cell lines, each spanning 38–4934 kb in size (median 747 kb), and 15 homozygous deletions in 13 cell lines, spanning 46–725 kb (median 183 kb).

Several localized high-level amplifications corresponded to known oncogenes, including *KRAS2* (12p12) [3,23] and *AKT2* (19q13) [24]; each of these genes was amplified in two pancreatic cancer cell lines. In addition, we identified several novel high-level amplifications, suggesting the location of as yet uncharacterized oncogenes. Nonrecurrent amplified loci

Table 2. Homozygous Deletions Identified by aCGH.

Cytoband	P Border	Q Border (nt)	Size (kb)	Cell Lines(s)	Remaining Lines with Single-Copy Loss	Gene Deletions Confirmed by PCR
6q25	157,305,093	157,562,885	258	MIA PaCa-2	0/19	ARID1B
8p23	1,717,413	1,894,213	177	MIA PaCa-2	13/19	CLN8, ARHGEF10
8p22	15,108,999	15,639,496	530	MIA PaCa-2	14/19	TUSC3
9p21*,†	21,845,793	21,984,872	139	BxPC-3, Capan-1, MIA PaCa-2, PANC-1, Panc 02.13, PL5, Su.86.86	6/13	CDKN2A
9q33 (a*)	112,922,979	113,392,575	470	BxPC-3	6/19	TNFSF15‡, TNFSF8, TNC, DEC1‡
10q22*	72,655,409	72,861,236	206	BxPC-3	4/19	CDH23‡
10q24	101,574,438	101,620,286	46	PL8	4/19	CHUK
11p15	11,942,981	12,118,344	175	BxPC-3	4/19	DKK3
16q23	78,558,946	78,688,790	130	HPAF-II	4/19	WWOX
18q21†	46,766,091	46,863,399	97	BxPC-3, CFPAC-1, Hs 766T, Panc 03.27, PL8	14/15	SMAD4
18q21*	49,277,732	50,003,145	725	MIA PaCa-2	18/19	DCC, MBD2
18q23	75,921,728	76,104,374	183	Colo-357	13/19	PARD6G
21q22	41,433,815	41,822,285	388	Panc 02.13	6/19	BACE2, MXI1, ANKRD3, PRDM15
21q22	41,822,119	42,524,687	703	BxPC-3	6/19	ANKRD3, PRDM15, ZNF295‡
Xp11	42,636,923	42,787,663	151	BxPC-3, MIA PaCa-2	6/18	MAOA

*Just over 0.25 ratio cutoff, but homozygous deletion was confirmed by PCR.
†Boundaries vary between cell lines; approximate site of common deletion is indicated.
‡Candidate TSG within deletion, but not represented on microarray.

included 6p21, 7q21, 11q22, 12p12 (proximal to *KRAS2*), 14q24, 17q12 (proximal to *ERBB2*), and 19q13 (proximal and distal to *AKT2*) (Table 1). Of the genes residing within these amplicons, several displayed correspondingly elevated expression and have plausible roles in tumorigenesis. Among these, the 7q21 amplicon "peak" [25] in AsPC-1 (Figure 1*A*) harbors *SMURF1*, an E3 ubiquitin ligase and negative regulator of TGFβ signaling [26]. Also residing in this amplicon are *ARPC1A* and *ARPC1B*, subunits of the ARP2/3 complex that controls actin polymerization and cell motility [27], and *TRRAP*, an essential cofactor for the transcriptional oncoproteins Myc and E2F [28]. We independently validated the 7q21 amplicon by interphase FISH (Figure 1*C*). Within the 11q22 amplicon in Colo-357 (Figure 1*B*), the apoptotic inhibitors *BIRC2* and *BIRC3* [29] were highly expressed. *TGFB3*, a ligand for TGFβ signaling [30], was found amplified at 14q24 in Panc 08.13.

We also identified numerous localized, presumptive homozygous deletions. Several such alterations corresponded to known TSGs, including *CDKN2A* (9p21), homozygously deleted in seven cell lines, and *SMAD4* (18q21), homozygously deleted in five cell lines (Table 2). Interestingly, the MIA PaCa-2 cell line harbors a homozygous deletion in the *DCC* gene, adjacent to but not affecting *SMAD4*, supporting a potential tumor-suppressor function for this gene [31]. In addition, we discovered several novel PCR-validated, localized homozygous deletions, suggesting new candidate TSGs at 6q25, 8p23, 8p22, 9q33, 10q22, 10q24, 11p15, 16q23, 18q23, 21q22, and Xp11 (Table 2). Among these, the 8p22 deletion in MIA PaCa-2 harbors *TUSC3*, a poorly characterized gene also homozygously deleted in a metastatic prostate cancer [32]. *TNC*, which modulates cell adhesion [33], and *TNFSF15*, a vascular endothelial inhibitor [34], reside within the 9q33 deletion in BxPC-3. The 10q23 deletion in PL8 harbors *CHUK* (also called *IKKA*), an activator of NF-κB signaling [35]. *DKK3* [36], an inhibitor of Wnt signaling [37], resides within the 11p15 deletion in BxPC-3 (Figure 2, *A* and *C*); an additional four cell lines displayed single-copy loss at

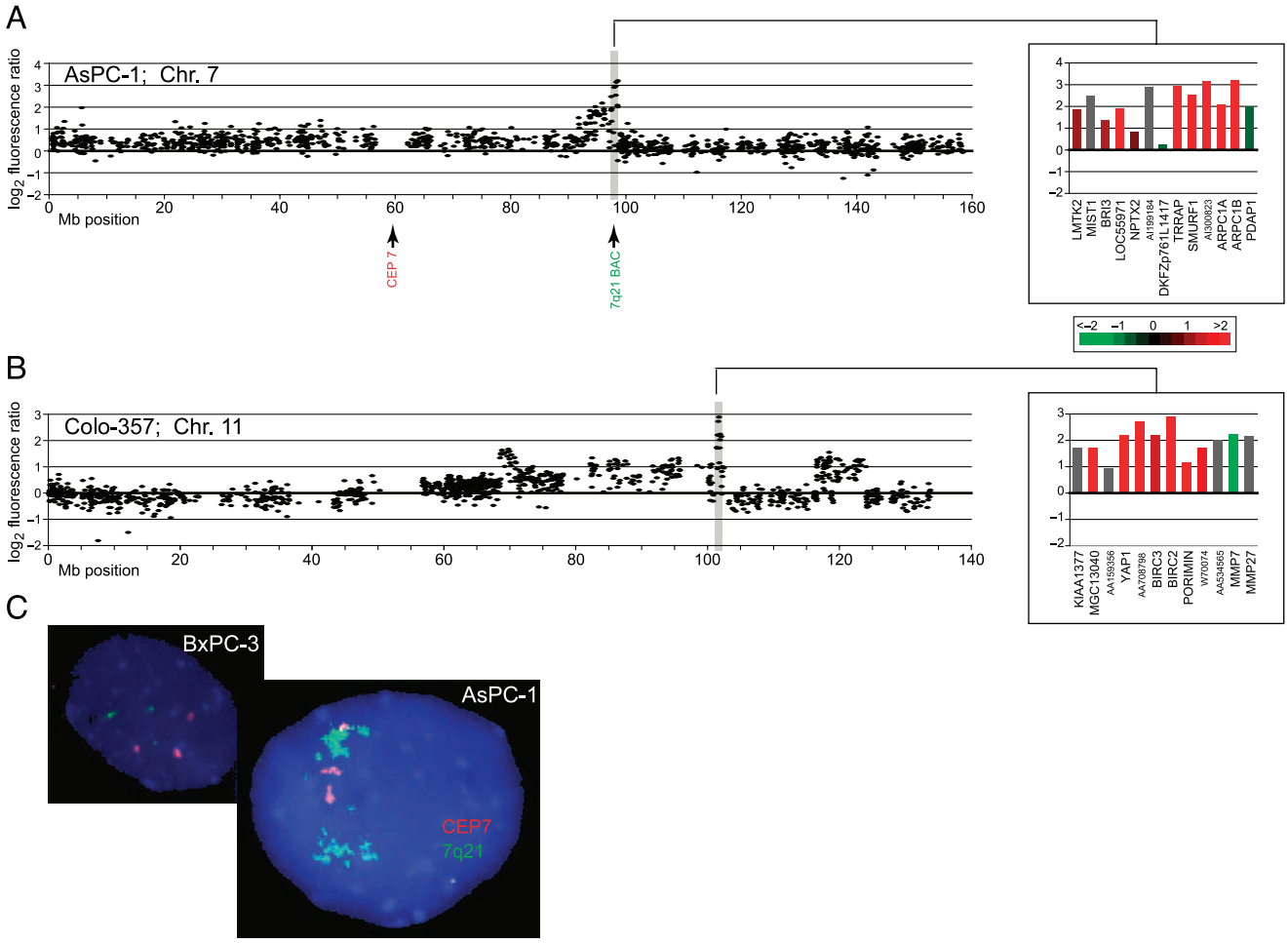

Figure 1. *Array CGH identifies localized DNA amplifications in pancreatic cancer. (A and B) Graphic displays of DNA copy number alteration for selected localized amplifications identified in pancreatic cancer cell lines. Test/reference fluorescence ratios are plotted on a $\log_2$ scale according to chromosome nucleotide (Megabase) position. Shaded regions highlight localized high-level amplifications. Insets display genes within highlighted amplicons, ordered by map position and color-coded according to mean-centered expression levels ($\log_2$ ratio scale indicated). (A) 7q21 amplicon in AsPC-1. (B) 11q22 amplicon in Colo-357. Complete genomewide profiles of DNA copy number alteration for the 22 pancreatic cancer cell lines are viewable in Figure W2. (C) FISH validation of 7q21 amplification in AsPC-1. Spectrum Orange chromosome 7 centromere probe detects three signals, whereas Spectrum Green 7q21 locus probe identifies multiple signal clusters indicative of DNA amplification. Nonamplified cell line BxPC-3 (triploid for chromosome 7) is shown for comparison.*

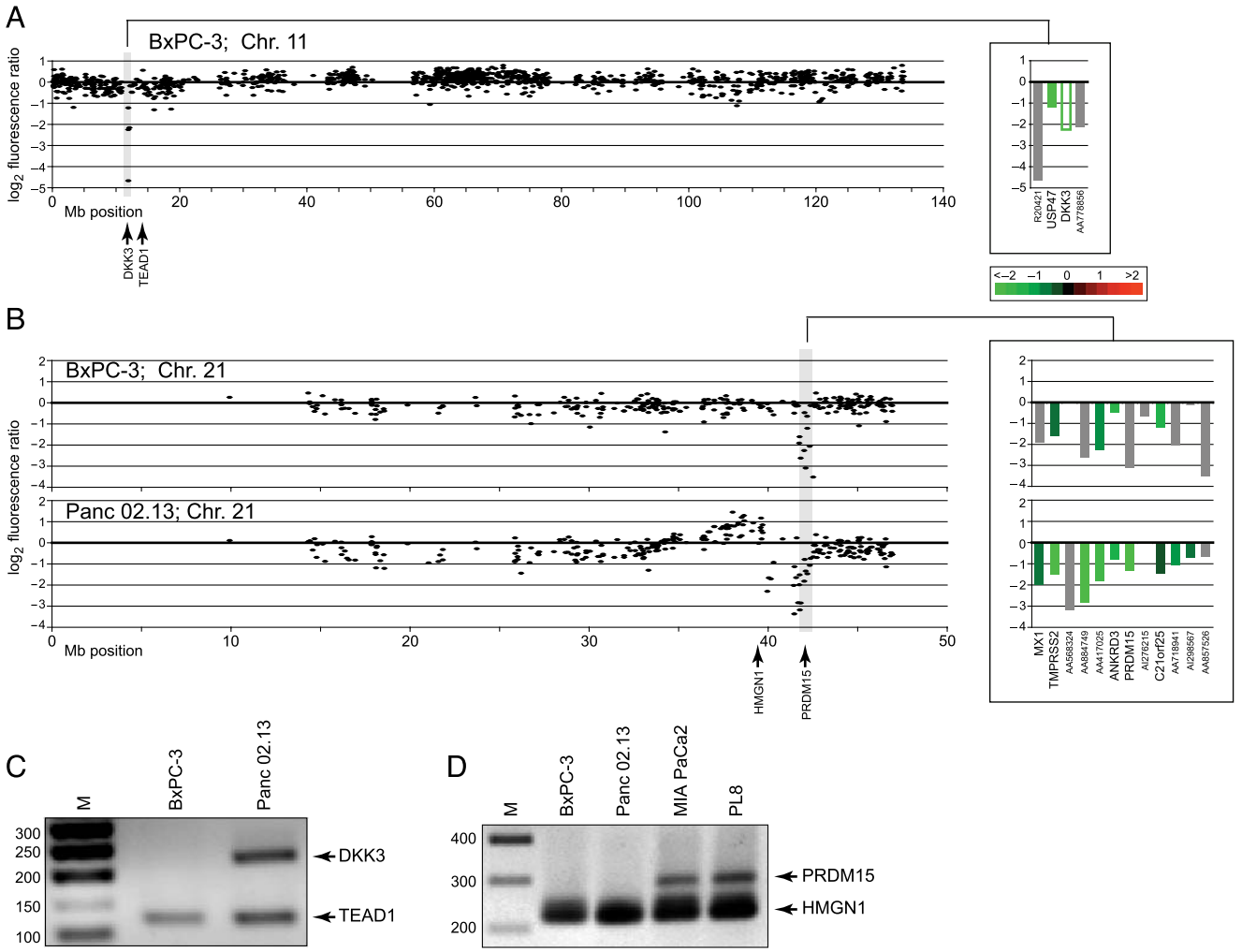

Figure 2. *Array CGH identifies localized homozygous DNA deletions in pancreatic cancer. (A and B) Test/reference fluorescence ratios are plotted on a $\log_2$ scale according to chromosome nucleotide (Megabase) position. Shaded regions highlight localized homozygous deletions. Insets display genes within highlighted deletions, ordered by map position and color-coded according to mean-centered expression levels ($\log_2$ ratio scale provided; unfilled green bar indicates measured intensity less than background). (A) 11p15 deletion in BxPC-3. (B) 21q22 deletion in BxPC-3 and Panc 02.13. (C) PCR validation of homozygous deletion at 11p15. DKK3, located within the homozygous deletion, is PCR-amplified in control cell line Panc 02.13 but not in BxPC-3. TEAD1, a control gene flanking the deletion, is PCR-amplified in both cell lines. (D) PCR validation of homozygous deletion at 21q22. PRDM15, located within the homozygous deletion, is PCR-amplified in control cell lines (MiaPaCa2 and PL8) but not in BxPC-3 and Panc 02.13. HMGN1, a control gene flanking the deletion, is PCR-amplified in all four cell lines.*

this site. The 21q22 locus (Figure 2, *B* and *D*), homozygously deleted in BxPC-3 and Panc 2.13 (with an additional six lines displaying single-copy loss), includes *PRDM15*, a putative histone methyltransferase, a class of enzymes frequently deregulated in human cancer [38], and *ANKRD3* (also called *RIP4*), another activator of NF-κB signaling [39].

Discussion

The main objective of our study was to use aCGH to identify localized DNA amplifications and deletions in pancreatic cancer, thereby defining the location of previously unrecognized candidate oncogenes and TSGs. In our aCGH analysis of 22 pancreatic adenocarcinoma cell lines, we identified 14 localized high-level amplifications and 15 localized homozygous deletions. Few of these localized aberrations had been identified earlier by conventional chromosome-based CGH [17,18]. Our findings therefore highlight the usefulness of high-resolution aCGH in discovering previously unrecognized DNA copy number aberrations. Notably, compared to broad chromosomal gains and losses, such highly localized aberrations also provide better opportunities to pinpoint and discover the underlying cancer genes.

As noted, the spectrum of gains and losses we observed was consistent with previous conventional CGH studies on primary pancreatic tumors. Furthermore, the observed subset of localized aberrations harboring known cancer genes (i.e., *KRAS2*, *AKT2*, *CDKN2A*, and *SMAD4*) has been well described in primary pancreatic tumors, suggesting that most novel aberrations are likely also to be found in primary tumor specimens. Nevertheless, as cells may acquire genetic changes during establishment and passage of cultures, the prevalence of these novel aberrations in primary pancreatic tumors will need to be determined.

Although our findings are, in general, consistent with previous chromosome-based CGH studies of the same

pancreatic cell lines, we did not identify the frequent gain of 1q reported by Tirado et al. [40], which may represent an artifact of the chromosome-based CGH method [41]. Three aCGH studies of pancreatic cell lines were also recently published. Holzmann et al. [42] surveyed 13 cell lines (five in common with our study) using BAC arrays with low-resolution coverage (498 clones), providing limited data for comparison. Aguirre et al. [43] profiled 24 cell lines (18 in common) using cDNA arrays (14,160 clones); however, their focus on broad low-level gains/losses, along with their not reporting which alterations were identified in which cell lines, makes meaningful comparisons difficult. Heidenblad et al. [44] studied 31 cell lines (nine in common) using BAC (3565 clones) and cDNA (25,468 clones) arrays, and their data were reported in sufficient detail to permit comparisons. Although our findings are in general agreement for the common set of cell lines investigated, we have identified several additional aberrations and candidate genes (Table W3), including the PCR-verified homozygous deletions at 11q and 21q (Figure 2). Discrepancies likely reflect the higher mapping resolution of our arrays and/or the different thresholds for calling gains and losses.

Our findings suggest several new candidate genes and pathways in pancreatic cancer. For example, *SMURF1* (7q21), amplified and overexpressed in AsPC-1, encodes an E3 ubiquitin ligase, which targets the degradation of TβRI receptor complex through its association with Smad7, thus suppressing the growth-inhibitory effects of TGFβ [26] (more frequently accomplished through *SMAD4* disruption). In contrast, our discovery of *TGFB3* (14q24) amplification in Panc 08.13 supports a possible tumorigenic role of Smad4-independent TGFβ signaling in pancreatic cancer [45]. Other alterations highlight the importance of inhibiting apoptosis, through amplification and overexpression of the antiapoptotic genes *BIRC2* and *BIRC3* (11q22), or possible modulation of NF-κB signaling [46] by deletion of *CHUK* (10q24) or *ANKRD3* (21q22). Interestingly, we identified *DKK3* (11p15), an inhibitor of Wnt signaling, within a highly localized homozygous deletion in the BxPC-3 cell line. Other cell lines exhibited single-copy loss and/or decreased expression of *DKK3*, suggesting that aberrant Wnt signaling may be common in pancreatic cancer. Although altered Wnt signaling contributes to the development of human cancers, most notably colorectal cancer [47], few reports to date have implicated Wnt signaling in the pathogenesis of pancreatic adenocarcinoma. However, consonant with our findings, Caca et al. [48] identified constitutive Tcf (the downstream effector of canonical Wnt signaling) transcriptional activity in two pancreatic cell lines.

In conclusion, our high-resolution genomewide aCGH study has led to the identification of numerous previously unrecognized localized DNA amplifications and deletions in pancreatic cancer. The expression levels, along with the known or inferred functions of the genes residing within these aberrations, suggest several new candidate oncogenes and TSGs. Our findings provide insight into the pathogenesis of pancreatic cancer, and may suggest new targets for improved therapies. Additional studies are required to characterize the functional role of identified genes in the development or progression of pancreatic cancer.

Acknowledgements

We thank Mike Fero and the staff of the Stanford Functional Genomics Facility for providing high-quality cDNA microarrays, and Gavin Sherlock and Catherine Ball of the Stanford Microarray Database group for providing outstanding database support.

References

[1] Jemal A, Tiwari RC, Murray T, Ghafoor A, Samuels A, Ward E, Feuer EJ, and Thun MJ (2004). Cancer statistics, 2004. *CA Cancer J Clin* **54,** 8–29.

[2] Bardeesy N and DePinho RA (2002). Pancreatic cancer biology and genetics. *Nat Rev Cancer* **2,** 897–909.

[3] Yamada H, Sakamoto H, Taira M, Nishimura S, Shimosato Y, Terada M, and Sugimura T (1986). Amplifications of both c-*Ki-ras* with a point mutation and c-*myc* in a primary pancreatic cancer and its metastatic tumors in lymph nodes. *Jpn J Cancer Res* **77,** 370–375.

[4] Solinas-Toldo S, Wallrapp C, Muller-Pillasch F, Bentz M, Gress T, and Lichter P (1996). Mapping of chromosomal imbalances in pancreatic carcinoma by comparative genomic hybridization. *Cancer Res* **56,** 3803–3807.

[5] Kamb A, Gruis NA, Weaver-Feldhaus J, Liu Q, Harshman K, Tavtigian SV, Stockert E, Day RS, Johnson BE, and Skolnick MH (1994). A cell cycle regulator potentially involved in genesis of many tumor types. *Science* **264,** 436–440.

[6] Hahn SA, Schutte M, Hoque AT, Moskaluk CA, da Costa LT, Rozenblum E, Weinstein CL, Fischer A, Yeo CJ, Hruban RH, et al. (1996). *DPC4*, a candidate tumor suppressor gene at human chromosome 18q21.1. *Science* **271,** 350–353.

[7] Kallioniemi A, Kallioniemi OP, Sudar D, Rutovitz D, Gray JW, Waldman F, and Pinkel D (1992). Comparative genomic hybridization for molecular cytogenetic analysis of solid tumors. *Science* **258,** 818–821.

[8] Pinkel D, Segraves R, Sudar D, Clark S, Poole I, Kowbel D, Collins C, Kuo WL, Chen C, Zhai Y, et al. (1998). High resolution analysis of DNA copy number variation using comparative genomic hybridization to microarrays. *Nat Genet* **20,** 207–211.

[9] Pollack JR, Perou CM, Alizadeh AA, Eisen MB, Pergamenschikov A, Williams CF, Jeffrey SS, Botstein D, and Brown PO (1999). Genome-wide analysis of DNA copy-number changes using cDNA microarrays. *Nat Genet* **23,** 41–46.

[10] Lucito R, West J, Reiner A, Alexander J, Esposito D, Mishra B, Powers S, Norton L, and Wigler M (2000). Detecting gene copy number fluctuations in tumor cells by microarray analysis of genomic representations. *Genome Res* **10,** 1726–1736.

[11] Schuler GD (1997). Pieces of the puzzle: expressed sequence tags and the catalog of human genes. *J Mol Med* **75,** 694–698.

[12] Pollack JR, Sorlie T, Perou CM, Rees CA, Jeffrey SS, Lonning PE, Tibshirani R, Botstein D, Borresen-Dale AL, and Brown PO (2002). Microarray analysis reveals a major direct role of DNA copy number alteration in the transcriptional program of human breast tumors. *Proc Natl Acad Sci USA* **99,** 12963–12968.

[13] Lapointe J, Li C, Higgins JP, van de Rijn M, Bair E, Montgomery K, Ferrari M, Egevad L, Rayford W, Bergerheim U, et al. (2004). Gene expression profiling identifies clinically relevant subtypes of prostate cancer. *Proc Natl Acad Sci USA* **101,** 811–816.

[14] Gollub J, Ball CA, Binkley G, Demeter J, Finkelstein DB, Hebert JM, Hernandez-Boussard T, Jin H, Kaloper M, Matese JC, et al. (2003). The Stanford Microarray Database: data access and quality assessment tools. *Nucleic Acids Res* **31,** 94–96.

[15] Wang P, Kim Y, Pollack J, Narasimhan B, and Tibshirani R (2005). A method for calling gains and losses in array CGH data. *Biostatistics* **6,** 45–58.

[16] Mahlamaki EH, Hoglund M, Gorunova L, Karhu R, Dawiskiba S, Andren-Sandberg A, Kallioniemi OP, and Johansson B (1997). Comparative genomic hybridization reveals frequent gains of 20q, 8q, 11q, 12p, and 17q, and losses of 18q, 9p, and 15q in pancreatic cancer. *Genes Chromosomes Cancer* **20,** 383–391.

[17] Curtis LJ, Li Y, Gerbault-Seureau M, Kuick R, Dutrillaux AM, Goubin G,

Fawcett J, Cram S, Dutrillaux B, Hanash S, et al. (1998). Amplification of DNA sequences from chromosome 19q13.1 in human pancreatic cell lines. *Genomics* **53,** 42–55.

[18] Ghadimi BM, Schrock E, Walker RL, Wangsa D, Jauho A, Meltzer PS, and Ried T (1999). Specific chromosomal aberrations and amplification of the *AIB1* nuclear receptor coactivator gene in pancreatic carcinomas. *Am J Pathol* **154,** 525–536.

[19] Schleger C, Arens N, Zentgraf H, Bleyl U, and Verbeke C (2000). Identification of frequent chromosomal aberrations in ductal adenocarcinoma of the pancreas by comparative genomic hybridization (CGH). *J Pathol* **191,** 27–32.

[20] Harada T, Okita K, Shiraishi K, Kusano N, Furuya T, Oga A, Kawauchi S, Kondoh S, and Sasaki K (2002). Detection of genetic alterations in pancreatic cancers by comparative genomic hybridization coupled with tissue microdissection and degenerate oligonucleotide primed polymerase chain reaction. *Oncology* **62,** 251–258.

[21] Peiper M, Nagoshi M, Patel D, Fletcher JA, Goedegebuure PS, and Eberlein TJ (1997). Human pancreatic cancer cells (MPanc-96) recognized by autologous tumor-infiltrating lymphocytes after *in vitro* as well as *in vivo* tumor expansion. *Int J Cancer* **71,** 993–999.

[22] Chen WH, Horoszewicz JS, Leong SS, Shimano T, Penetrante R, Sanders WH, Berjian R, Douglass HO, Martin EW, and Chu TM (1982). Human pancreatic adenocarcinoma: *in vitro* and *in vivo* morphology of a new tumor line established from ascites. *In Vitro* **18,** 24–34.

[23] Heidenblad M, Jonson T, Mahlamaki EH, Gorunova L, Karhu R, Johansson B, and Hoglund M (2002). Detailed genomic mapping and expression analyses of 12p amplifications in pancreatic carcinomas reveal a 3.5-Mb target region for amplification. *Genes Chromosomes Cancer* **34,** 211–223.

[24] Cheng JQ, Ruggeri B, Klein WM, Sonoda G, Altomare DA, Watson DK, and Testa JR (1996). Amplification of AKT2 in human pancreatic cells and inhibition of AKT2 expression and tumorigenicity by antisense RNA. *Proc Natl Acad Sci USA* **93,** 3636–3641.

[25] Albertson DG, Ylstra B, Segraves R, Collins C, Dairkee SH, Kowbel D, Kuo WL, Gray JW, and Pinkel D (2000). Quantitative mapping of amplicon structure by array CGH identifies CYP24 as a candidate oncogene. *Nat Genet* **25,** 144–146.

[26] Ebisawa T, Fukuchi M, Murakami G, Chiba T, Tanaka K, Imamura T, and Miyazono K (2001). *Smurf1* interacts with transforming growth factor-beta type I receptor through Smad7 and induces receptor degradation. *J Biol Chem* **276,** 12477–12480.

[27] Welch MD (1999). The world according to Arp: regulation of actin nucleation by the Arp2/3 complex. *Trends Cell Biol* **9,** 423–427.

[28] McMahon SB, Van Buskirk HA, Dugan KA, Copeland TD, and Cole MD (1998). The novel ATM-related protein *TRRAP* is an essential cofactor for the c-Myc and E2F oncoproteins. *Cell* **94,** 363–374.

[29] Liston P, Fong WG, and Korneluk RG (2003). The inhibitors of apoptosis: there is more to life than Bcl2. *Oncogene* **22,** 8568–8580.

[30] Shi Y and Massague J (2003). Mechanisms of TGF-beta signaling from cell membrane to the nucleus. *Cell* **113,** 685–700.

[31] Hilgers W, Song JJ, Haye M, Hruban RR, Kern SE, and Fearon ER (2000). Homozygous deletions inactivate DCC, but not MADH4/DPC4/SMAD4, in a subset of pancreatic and biliary cancers. *Genes Chromosomes Cancer* **27,** 353–357.

[32] MacGrogan D, Levy A, Bova GS, Isaacs WB, and Bookstein R (1996). Structure and methylation-associated silencing of a gene within a homozygously deleted region of human chromosome band 8p22. *Genomics* **35,** 55–65.

[33] Chiquet-Ehrismann R and Chiquet M (2003). Tenascins: regulation and putative functions during pathological stress. *J Pathol* **200,** 488–499.

[34] Zhai Y, Ni J, Jiang GW, Lu J, Xing L, Lincoln C, Carter KC, Janat F, Kozak D, Xu S, et al. (1999). VEGI, a novel cytokine of the tumor necrosis factor family, is an angiogenesis inhibitor that suppresses the growth of colon carcinomas *in vivo*. *FASEB J* **13,** 181–189.

[35] Regnier CH, Song HY, Gao X, Goeddel DV, Cao Z, and Rothe M (1997). Identification and characterization of an IkappaB kinase. *Cell* **90,** 373–383.

[36] Krupnik VE, Sharp JD, Jiang C, Robison K, Chickering TW, Amaravadi L, Brown DE, Guyot D, Mays G, Leiby K, et al. (1999). Functional and structural diversity of the human *Dickkopf* gene family. *Gene* **238,** 301–313.

[37] Hoang BH, Kubo T, Healey JH, Yang R, Nathan SS, Kolb EA, Mazza B, Meyers PA, and Gorlick R (2004). Dickkopf 3 inhibits invasion and motility of Saos-2 osteosarcoma cells by modulating the Wnt-beta–catenin pathway. *Cancer Res* **64,** 2734–2739.

[38] Schneider R, Bannister AJ, and Kouzarides T (2002). Unsafe SETs: histone lysine methyltransferases and cancer. *Trends Biochem Sci* **27,** 396–402.

[39] Meylan E, Martinon F, Thome M, Gschwendt M, and Tschopp J (2002). RIP4 (DIK/PKK), a novel member of the RIP kinase family, activates NF-kappa B and is processed during apoptosis. *EMBO Rep* **3,** 1201–1208.

[40] Tirado CA, Sandberg AA, and Stone JF (1999). Identification of a novel amplicon at 1q31 in pancreatic cancer cell lines. *Cancer Genet Cytogenet* **113,** 110–114.

[41] Kallioniemi OP, Kallioniemi A, Piper J, Isola J, Waldman FM, Gray JW, and Pinkel D (1994). Optimizing comparative genomic hybridization for analysis of DNA sequence copy number changes in solid tumors. *Genes Chromosomes Cancer* **10,** 231–243.

[42] Holzmann K, Kohlhammer H, Schwaenen C, Wessendorf S, Kestler HA, Schwoerer A, Rau B, Radlwimmer B, Dohner H, Lichter P, et al. (2004). Genomic DNA-chip hybridization reveals a higher incidence of genomic amplifications in pancreatic cancer than conventional comparative genomic hybridization and leads to the identification of novel candidate genes. *Cancer Res* **64,** 4428–4433.

[43] Aguirre AJ, Brennan C, Bailey G, Sinha R, Feng B, Leo C, Zhang Y, Zhang J, Gans JD, Bardeesy N, et al. (2004). High-resolution characterization of the pancreatic adenocarcinoma genome. *Proc Natl Acad Sci USA* **101,** 9067–9072.

[44] Heidenblad M, Schoenmakers EF, Jonson T, Gorunova L, Veltman JA, van Kessel AG, and Hoglund M (2004). Genome-wide array-based comparative genomic hybridization reveals multiple amplification targets and novel homozygous deletions in pancreatic carcinoma cell lines. *Cancer Res* **64,** 3052–3059.

[45] Subramanian G, Schwarz RE, Higgins L, McEnroe G, Chakravarty S, Dugar S, and Reiss M (2004). Targeting endogenous transforming growth factor beta receptor signaling in SMAD4-deficient human pancreatic carcinoma cells inhibits their invasive phenotype 1. *Cancer Res* **64,** 5200–5211.

[46] Kucharczak J, Simmons MJ, Fan Y, and Gelinas C (2003). To be, or not to be: NF-kappaB is the answer—role of Rel/NF-kappaB in the regulation of apoptosis. *Oncogene* **22,** 8961–8982.

[47] Karim R, Tse G, Putti T, Scolyer R, and Lee S (2004). The significance of the Wnt pathway in the pathology of human cancers. *Pathology* **36,** 120–128.

[48] Caca K, Kolligs FT, Ji X, Hayes M, Qian J, Yahanda A, Rimm DL, Costa J, and Fearon ER (1999). Beta- and gamma-catenin mutations, but not E-cadherin inactivation, underlie T-cell factor/lymphoid enhancer factor transcriptional deregulation in gastric and pancreatic cancer. *Cell Growth Differ* **10,** 369–376.

Table W1. Pancreatic Cancer Cell Lines.

Cell Line	Gender	Origin	Source	Reference
AsPC-1	Female	Nude mouse xenograft of ascites cells from patient with pancreatic adenocarcinoma	ATCC	Chen, W.H. et al. (1982). *In Vitro*, 18, 24–34.
BxPC-3	Female	Pancreatic adenocarcinoma	ATCC	Tan, M.H. et al. (1986). *Cancer Invest*, 4, 15–23.
Capan-1	Male	Liver metastasis of pancreatic adenocarcinoma	ATCC	Fogh, J. et al. (1977). *J Natl Cancer Inst*, 58, 209–14.
Capan-2	Male	Pancreatic adenocarcinoma	ATCC	Kyriazis, A.A. et al. (1986). *Cancer Res*, 46, 5810–5.
CFPAC-1	Male	Liver metastasis of pancreatic ductal adenocarcinoma	ATCC	Schoumacher, R.A. et al. (1990). *Proc Natl Acad Sci U S A*, 87, 4012–6.
Colo-357	Female	Lymph node metastasis of pancreatic adenocarcinoma	Dr. Caroline Hill, London Research Institute	Morgan, R.T. et al. (1980). *Int J Cancer*, 25, 591–8.
HPAC	Female	Nude mouse xenograft of a moderate to well differentiated pancreatic adenocarcinoma of ductal origin	ATCC	Gower, Jr., W.R. et al. (1994). In Vitro Cell. Dev. Biol. 30A: 151–161
HPAF-II	Male	Peritoneal ascites from pancreatic adenocarcinoma with mets to liver, diaphragm and lymph nodes	ATCC	Kim, Y.W. et al. (1989). *Pancreas*, 4, 353–62.
Hs 766T	Male	Lymph node metastasis of pancreatic cancer	ATCC	Owens, R.B. et al. (1976). *J Natl Cancer Inst*, 56, 843–9.
MIA PaCa-2	Male	Primary pancreatic carcinoma	ATCC	Yunis, A.A., et al. (1977). *Int J Cancer*, 19, 218–35.
MPanc96	Male	Primary malignant pancreatic adenocarcinoma	ATCC	Peiper, M. et al. (1997). *Int J Cancer*, 71, 993–9
PANC-1	Female	Primary pancreatic adenocarcinoma from pancreatic duct	ATCC	Lieber, M. et al. (1975). *Int J Cancer*, 15, 741–7.
Panc 02.03	Female	Primary pancreatic adenocarcinoma from head of pancreas	ATCC	Jaffee, E.M. et al. (1998). *Cancer J Sci Am*, 4, 194–203.
Panc 02.13	Female	Primary pancreatic adenocarcinoma from head of pancreas	ATCC	Jaffee, E.M. et al. (1998). *Cancer J Sci Am*, 4, 194–203.
Panc 03.27	Female	Primary pancreatic adenocarcinoma from head of pancreas	ATCC	Jaffee, E.M. et al. (1998). *Cancer J Sci Am*, 4, 194–203.
Panc 08.13	Male	Primary pancreatic adenocarcinoma from head of pancreas	ATCC	Jaffee, E.M. et al. (1998). *Cancer J Sci Am*, 4, 194–203.
Panc 10.05	Male	Primary pancreatic adenocarcinoma from head of pancreas	ATCC	Jaffee, E.M. et al. (1998). *Cancer J Sci Am*, 4, 194–203.
PL45	Male	Poorly differentiated primary pancreatic adenocarcinoma of ductal origin	ATCC	Jaffee, E.M. et al. (1998). *Cancer J Sci Am*, 4, 194–203.
PL5	Male	Primary pancreatic adenocarcinoma	Dr. Anirban Maitra, Johns Hopkins University	Jaffee, E.M. et al. (1998). *Cancer J Sci Am*, 4, 194–203.
PL8	Male	Primary pancreatic adenocarcinoma	Dr. Anirban Maitra, Johns Hopkins University	Jaffee, E.M. et al. (1998). *Cancer J Sci Am*, 4, 194–203.
SU.86.86	Female	Liver metastasis of a pancreatic ductal carcinoma	ATCC	Drucker, B.J. et al. (1988). *In Vitro Cell Dev Biol*, 24, 1179–87.
SW 1990	Male	Spleen metastasis of a grade II pancreatic adenocarcinoma	ATCC	Kyriazis, A.A. et al. (1986). *Cancer Res*, 46, 5810–5.

Table W2. PCR Primer Sequences for Validation of Homozygous Deletion.

Cytoband	Gene	Cell Line(S)	Forward Primer	Reverse Primer	SIZE (bp)
6q25	ARID1B	MIA PaCa-2	TCCGAACATATCCAGTATTCCA	CAACGGTCAGACTCTGCGTA	111
8p23	CLN8	MIA PaCa-2	ACACTGTTCCGAGAGTTCCATA	CTGATGATGAGTCCCAAGGT	278
8p23	ARHGEF10	MIA PaCa-2	ACTTTATTGATGAAGTCAGACAGCA	CTTAGCCAAATATGTTCTAGGTTGC	102
8p22	TUSC3	MIA PaCa-2	GATTGAGGATTTGATGGAAAGC	TCCTCTGGGAATCCAGACTT	129
9p21	CDKN2A	BxPC-3, Capan-1, MIA PaCa-2, PANC-1, Panc 02.13, PL5, Su.86.86	TTTATTCATTTGCTTGTGGCC	GGTCCCGATTTAGAAGGAGC	120
9q33	TNFSF15	BxPC-3	CTCTGCACTGGGAACATGAA	TTGGCTCAGGGTAGCTGTCT	228
9q33	TNFSF8	BxPC-3	TATTTCATAGAGGAGACCTAGGAGG	CAAATCAGCAGTGGTGGTATG	125
9q33	TNC	BxPC-3	GCCTCACCTCCTCTGTGATT	AAAAAGGGATGGCTTCCAAT	271
9q33	DEC1	BxPC-3	ATAAGTAATCACAAGGTACAGGGAA	CTTTTGGAGAACCATATGTTAAATC	135
10q22	CDH23	BxPC-3	TGGGAATTCTCAACAGGTCC	ACGGGGAGCATCTACCAAG	161
10q24	CHUK	PL8	TTCTCTGAAACCCTTGGGG	TGCTGCTTGATGATGAGAGG	145
11p15	DKK3	BxPC-3	CTTTAAACTTTAAGAACTCTGG	ACTTAGGTAATTGTAGGGC	231
16q23	WWOX	HPAF-II	TGAGGGCAGGATACCACTTC	CAGAGACTGAGATGGCCACA	394
18q21	SMAD4	BxPC-3, CFPAC-1, Hs 766T, Panc 03.27, PL8	TCCTTCCCCAGATGACCATAGT	GGCAGGGTGTGGTGTGTAAAGGG	164
18q21	DCC	MIA PaCa-2	GGCCCACTCTTCCTAAGACC	TTACACAGCGCCAGTCAATC	202
18q21	MBD2	MIA PaCa-2	GAATGAGGTGGATGGTAAATCA	TGTGACTTGTTTGTCTGCTTCA	131
18q23	PARD6G	Colo-357	GAGGGACGCAGATGAGAAAA	CAGGGCACATTTAGGAAGGA	135
21q22	BACE2	Panc 02.13	GAACCCCGCACTCCTACATA	TGCTCTGGTGCATTTTGAAG	119
21q22	MX1	BxPC-3, Panc 02.13	GCAAGGTGGAGCGATTC	GTTAGCCGTGGTGATTTAGC	158
21q22	ANKRD3	BxPC-3, Panc 02.13	TGGAAAAGTATCCTGCCCAC	TCACCTGTGTCCCATAGGGT	164
21q22	PRDM15	BxPC-3, Panc 02.13	ACGGGTCACAGCACCTTT	ATGCTCTAGCGTGTGACGTG	291
21q22	ZNF295	BxPC-3	AGCCGGAGACTTCGCATAGT	AGTTTGAGTGTCTGCGGGAG	277
Xp11	MAOA	BxPC-3	TTAAATGGTCTCGGGAAGG	GCCCAATGACACAGCCTTT	488

Table W2. (*continued*)

Flanking Gene	Forward Primer	Reverse Primer	Size (bp)	Annealing Temp
SYNJ2	TTGCAGCTTTCCTTCCCAAT	GACCCCAAGCCTAGTCCCTT	243	57
MYOM2	TATACCCGTCTAAGGGAGAAAGC	GTGTGTTGTCTGCCAACCC	111	56
CSMD1	TGATGCCGAGGTCACTG	CCTCTTGGAGTATTAAAGTGGAAC	141	58
CTSB	GGAGCCCTTTGGAGAAC	TGAGCCGCGTCATTAG	201	55
ACO1	AATGTGTTCTCCCAAACCG	CAGAGTGAATCATCCAGACTCC	167	56
CIP98	TGGATGAATTCTCGAGTGACC	CCCAGGACAAGTGGGTTGG	167	56
CIP98	TGGATGAATTCTCGAGTGACC	CCCAGGACAAGTGGGTTGG	167	58
CIP98	TGGATGAATTCTCGAGTGACC	CCCAGGACAAGTGGGTTGG	167	55
CIP98	TGGATGAATTCTCGAGTGACC	CCCAGGACAAGTGGGTTGG	167	56
PCDB	AGCTGAGGAGCCCTTACC	TATTGTTGCTGGGAAGTTGC	210	56
PAX2	GACCGCCACTAGTTACCGC	GCTCCACCCGTCCTGTCC	205	57
TEAD1	GATAAGGGGTGAAGTTTTCT	TGCTTGGTAGAAGTGTCC	122	53
MAF	AAGCACATAGGAACAACACGC	TTTCAGGGACTGACATCCTG	166	59
MALT1	ACCTTCTGCAACTTCATCCAGTA	GTAACCACCATTCTGCTGGG	249	59
MALT1	ACCTTCTGCAACTTCATCCAGTA	GTAACCACCATTCTGCTGGG	249	58
MALT1	ACCTTCTGCAACTTCATCCAGTA	GTAACCACCATTCTGCTGGG	249	57
NFATC1	ACTGTGTGATGTCCCGTTAGTGA	TATTCCTAAAGGTGCCTGCAAAA	290	58
HMGN1	CTGAGATTTTATTGGTTGAGGATCA	AACTGGTGGGCCGTATGTAA	216	57
HMGN1	CTGAGATTTTATTGGTTGAGGATCA	AACTGGTGGGCCGTATGTAA	216	58
HMGN1	CTGAGATTTTATTGGTTGAGGATCA	AACTGGTGGGCCGTATGTAA	216	57
HMGN1	CTGAGATTTTATTGGTTGAGGATCA	AACTGGTGGGCCGTATGTAA	216	57
HMGN1	CTGAGATTTTATTGGTTGAGGATCA	AACTGGTGGGCCGTATGTAA	216	58
CHST7	ATGATTACAAAAACGCCAGACA	AATAGCTCCGTCTCCCTTTACC	132	56

Table W3. Comparison to Aberrations identified by Heidenblad et al. [44].

Cytoband	P-Border (nt)	Q-Border (nt)	Size (Kb)	Cell Line	Selected Candidate Genes
Amplifications					
6p21*	32,043,837	32,410,885	367	SW 1990	STK19, TNXB, PBX2, NOTCH4
6p21*	32,827,514	32,865,810	38	SW 1990	TAP1
7q21*	93,671,907	98,605,497	4,934	AsPC-1	TRRAP, SMURF1, ARPC1A, ARPC1B
11q13§	69,241,850	70,008,988	767	Colo-357	CCND1, EMS1
11q22§	101,406,590	102,133,375	727	Colo-357	YAP1, BIRC2, BIRC3, MMP7, MMP27
12p12†	14,926,093	15,186,368	260	Su.86.86	
12p12†	25,253,402	26,380,345	1,127	Su.86.86	KRAS2
12p11‡	25,253,402	27,366,920	2,114	HPAF-II	KRAS2, FGHR1OP2, STK38L
14q24§	74,414,776	74,540,126	125	Panc 08.13	TGFB3
17q12‡	36,065,530	36,106,569	41	CFPAC-1	
19q13†	39,957,195	40,808,091	851	Su.86.86	USF2
19q13*	43,616,179	45,546,133	1,930	PANC-1	eIF3k, AKT2
19q13†	43,997,907	46,073,560	2,076	Su.86.86	AKT2
19q13*	55,171,535	55,539,817	368	Su.86.86	ZNF473
Deletions					
6q25§	157,305,093	157,562,885	258	MIA PaCa-2	
8p23§	1,717,413	1,894,213	177	MIA PaCa-2	ARID1B
8p22§	15,108,999	15,639,496	530	MIA PaCa-2	CLN8, ARHGEF10
9p21*	21,845,793	21,984,872	139	BxPC-3, Capan-1, MIA PaCa-2, PANC-1, Panc 02.13, PL5, Su.86.86	TUSC3
9q33*	112,922,979	113,392,575	470	BxPC-3	CDKN2A
10q22*	72,655,409	72,861,236	206	BxPC-3	TNFSF15, TNFSF8, TNC, DEC1
10q24§	101,574,438	101,620,286	46	PL8	CDH23
11p15‡	11,942,981	12,118,344	175	BxPC-3	CHUK
16q23‡	78,558,946	78,688,790	130	HPAF-II	DKK3
18q21*	46,766,091	46,863,399	97	BxPC-3, CFPAC-1, Hs 766T, Panc 03.27, PL8	WWOX
18q21‡	49,277,732	50,003,145	725	MIA PaCa-2	SMAD4
18q23§	75,921,728	76,104,374	183	Colo-357	DCC, MBD2
21q22§	41,433,815	41,822,285	388	Panc 02.13	PARD6G
21q22‡	41,822,119	42,524,687	703	BxPC-3	BACE2, MXI1, ANKRD3, PRDM15
Xp11‡	42,636,923	42,787,663	151	BxPC-3, MIA PaCa-2	ANKRD3, PRDM15, ZNF295 MAOA

*Aberration also identified by Heidenblad et al.
† Aberration identified by Heidenblad et al., but not resolved into two distinct amplicons as here.
‡ Aberration not identified by Heidenblad et al.
§ Cell line not studied by Heidenblad et al.

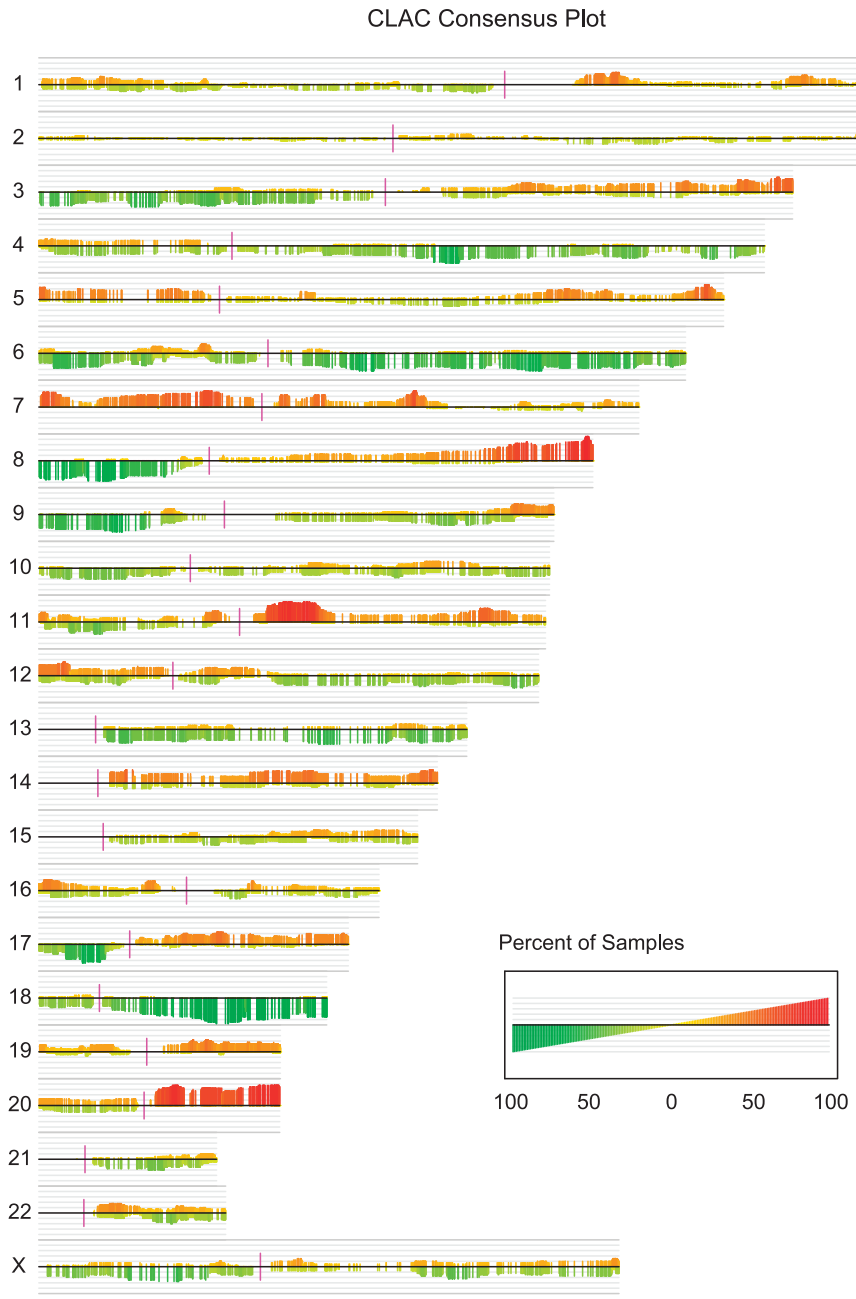

Figure W1. *Consensus plot of DNA copy number alterations identified with the CLuster Along Chromosomes (CLAC) method (15) using the CGH-Miner software (http://www-stat.stanford.edu/~wp57/CGH-Miner). Frequencies of gain and loss are plotted for each gene locus using a colorimetric and height scale (indicated). Cell lines Panc 10.05 and MPanc-96 are excluded from this frequency plot, so as to not over-represent duplicated samples (see main text).*

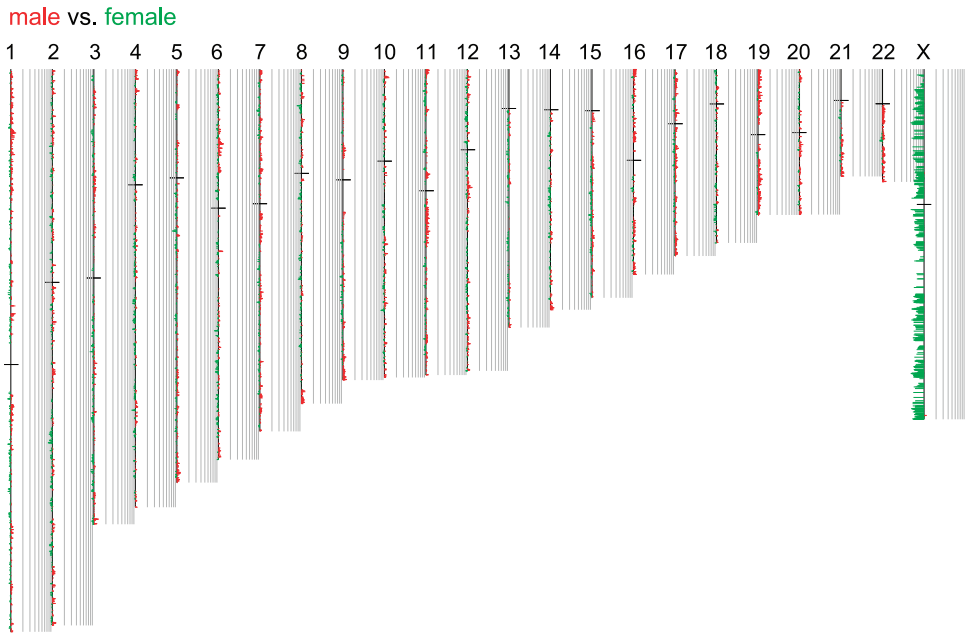

Figure W2. *Genome-wide aCGH profiles of DNA copy number alteration for the 22 pancreatic cancer cell lines. A normal male-female DNA control hybridization is also provided. Fluorescence ratios are plotted on a log_{10} scale, here as a moving average of 5 adjacent genes, according to chromosome position where red and green indicate positive and negative ratios, respectively. Centromeres are indicated by black bar.*

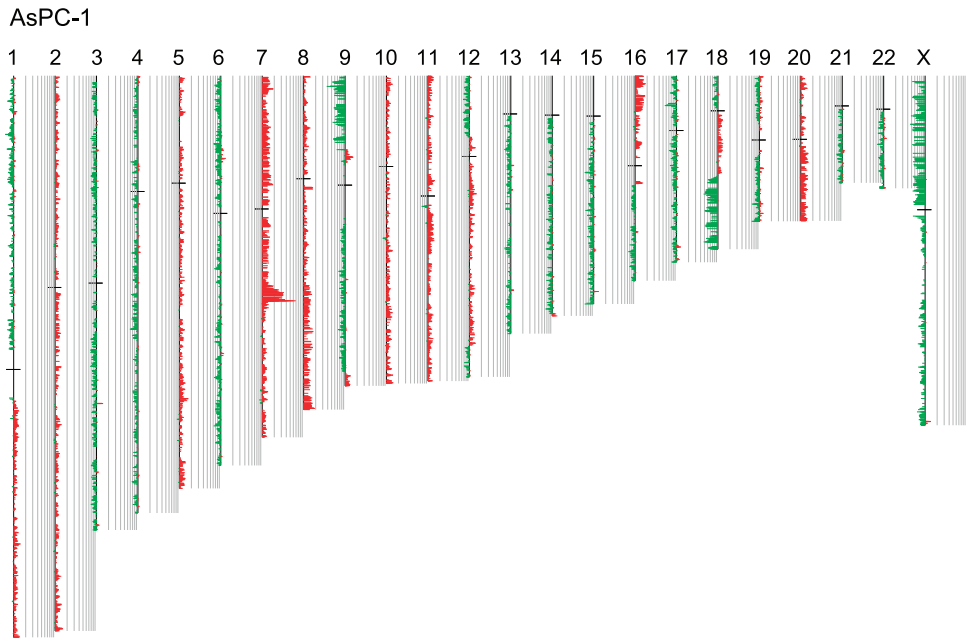

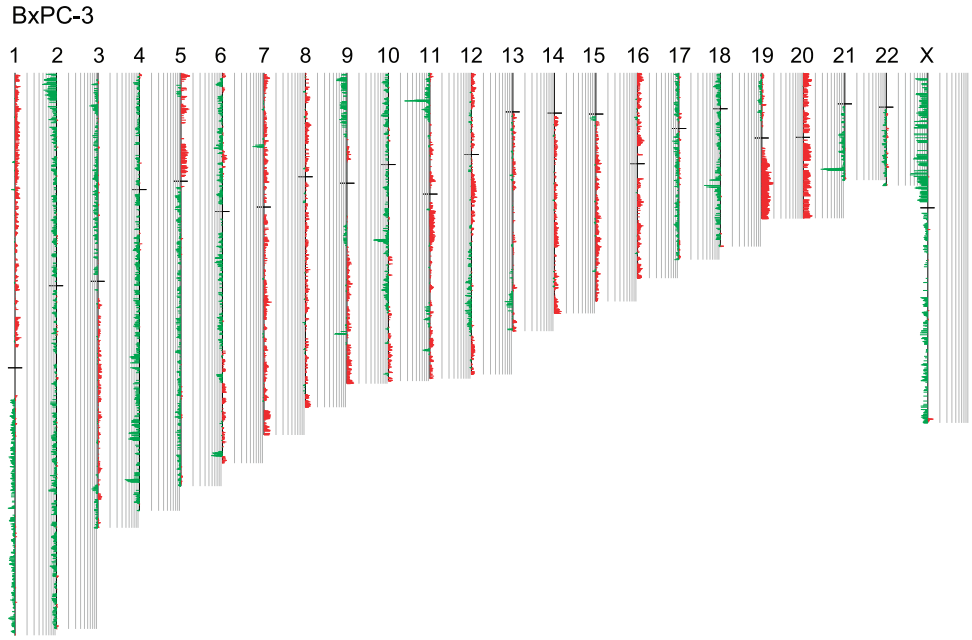
BxPC-3
1 2 3 4 5 6 7 8 9 10 11 12 13 14 15 16 17 18 19 20 21 22 X

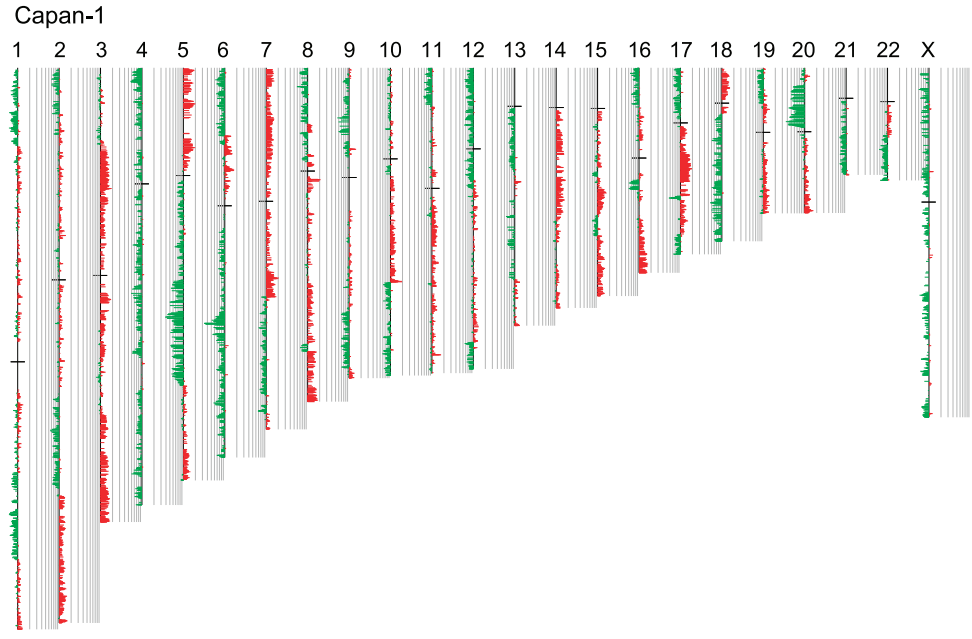
Capan-1
1 2 3 4 5 6 7 8 9 10 11 12 13 14 15 16 17 18 19 20 21 22 X

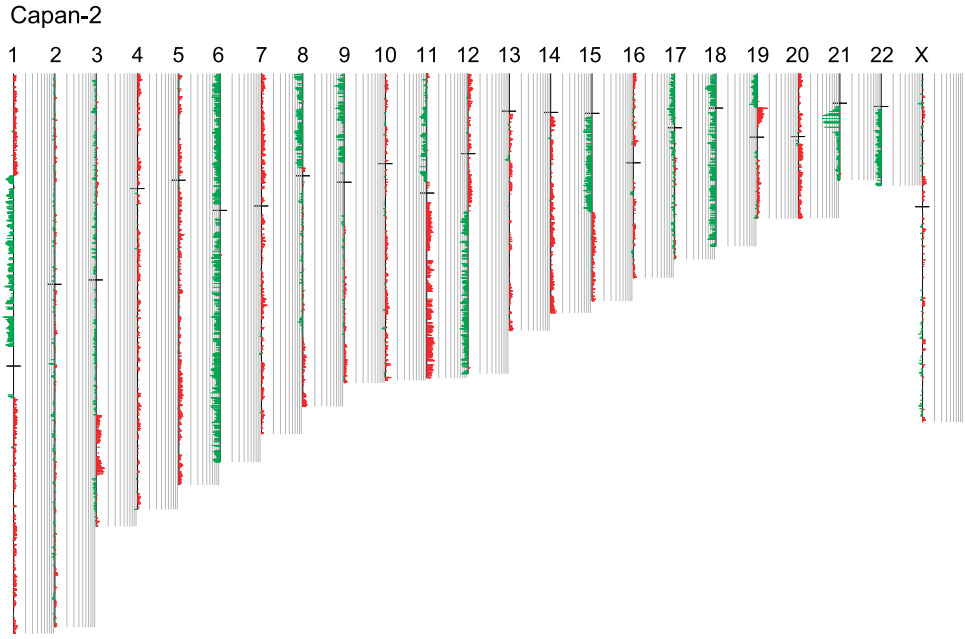
Capan-2
1 2 3 4 5 6 7 8 9 10 11 12 13 14 15 16 17 18 19 20 21 22 X

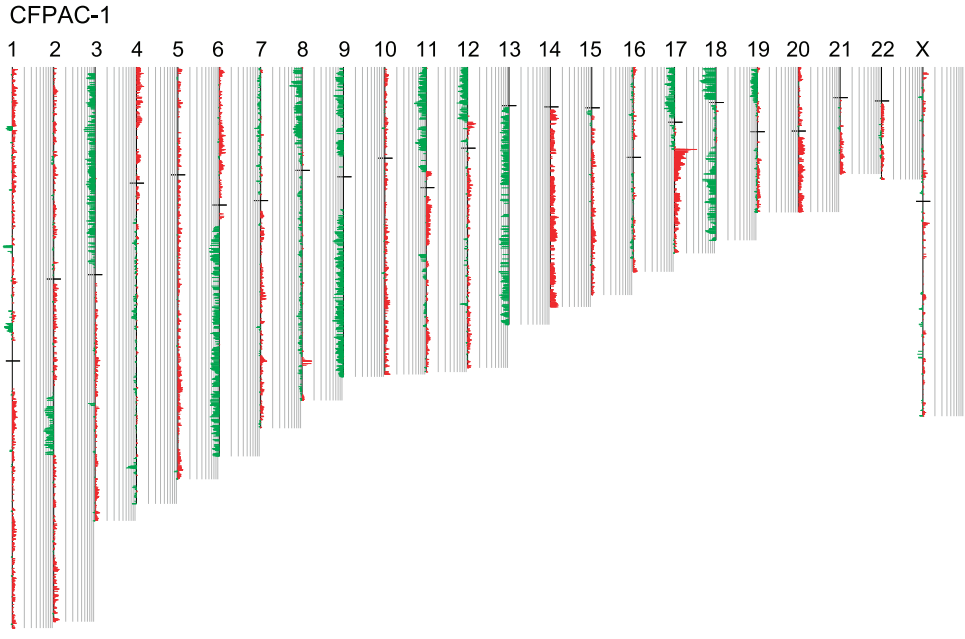
CFPAC-1
1 2 3 4 5 6 7 8 9 10 11 12 13 14 15 16 17 18 19 20 21 22 X

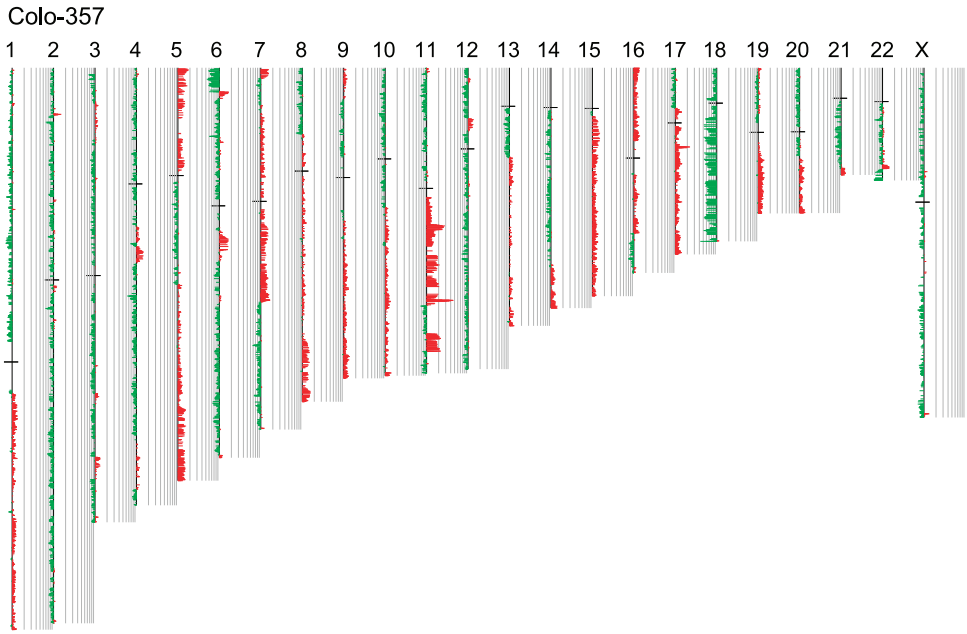
Colo-357
1 2 3 4 5 6 7 8 9 10 11 12 13 14 15 16 17 18 19 20 21 22 X

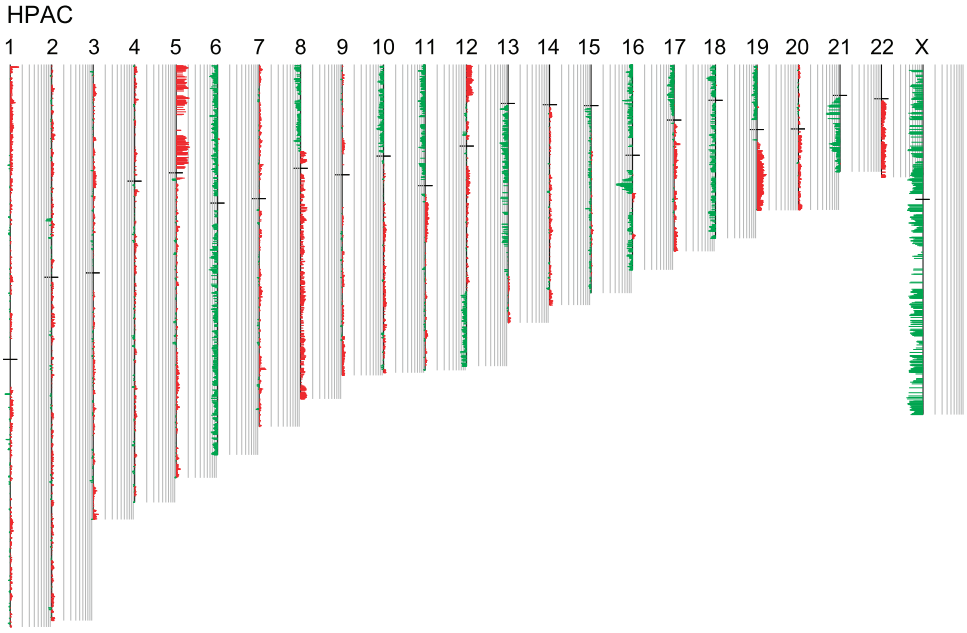
HPAC
1 2 3 4 5 6 7 8 9 10 11 12 13 14 15 16 17 18 19 20 21 22 X

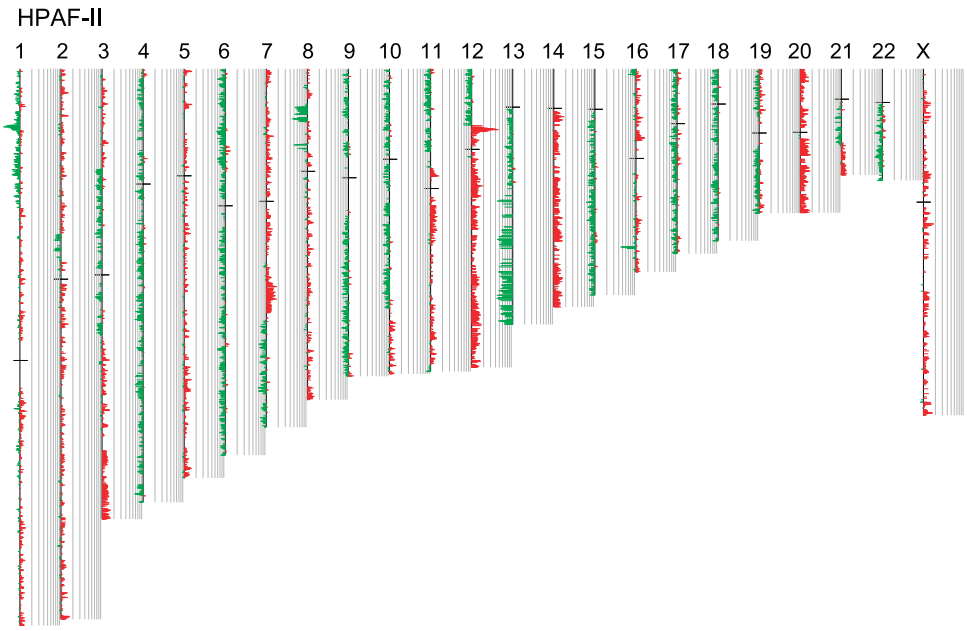
HPAF-II
1 2 3 4 5 6 7 8 9 10 11 12 13 14 15 16 17 18 19 20 21 22 X

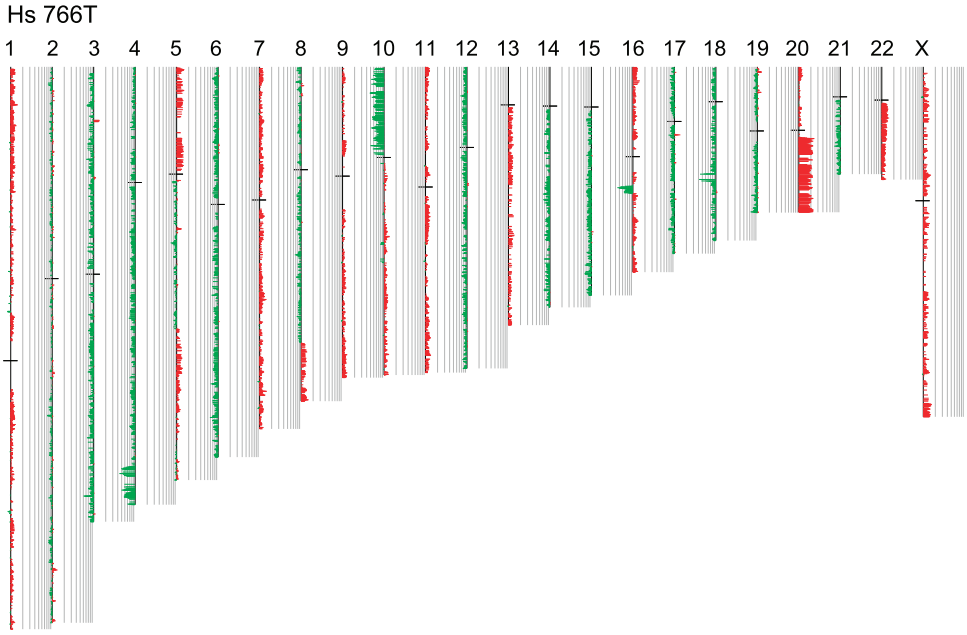
Hs 766T
1 2 3 4 5 6 7 8 9 10 11 12 13 14 15 16 17 18 19 20 21 22 X

MIA PaCa-2

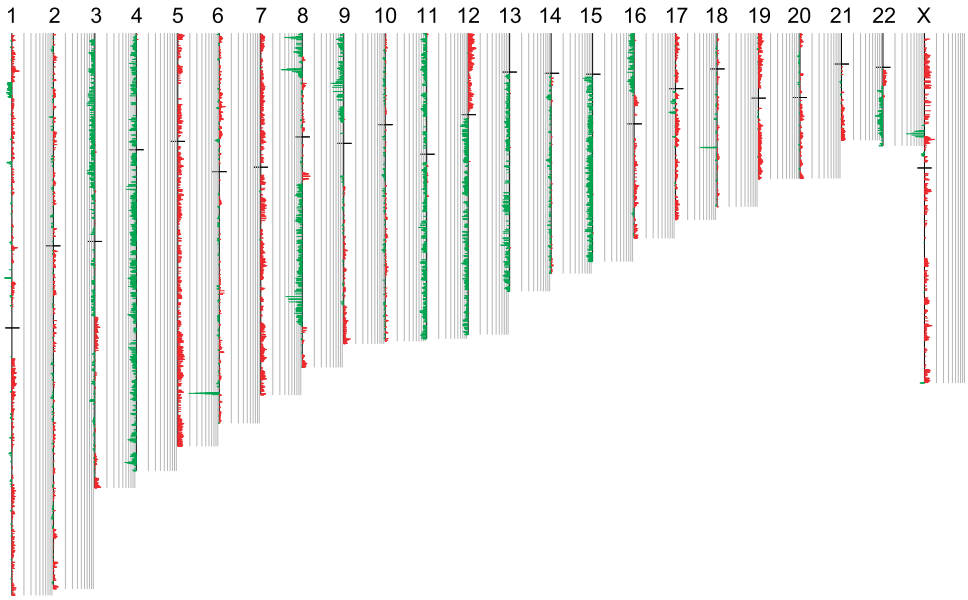

MPanc96

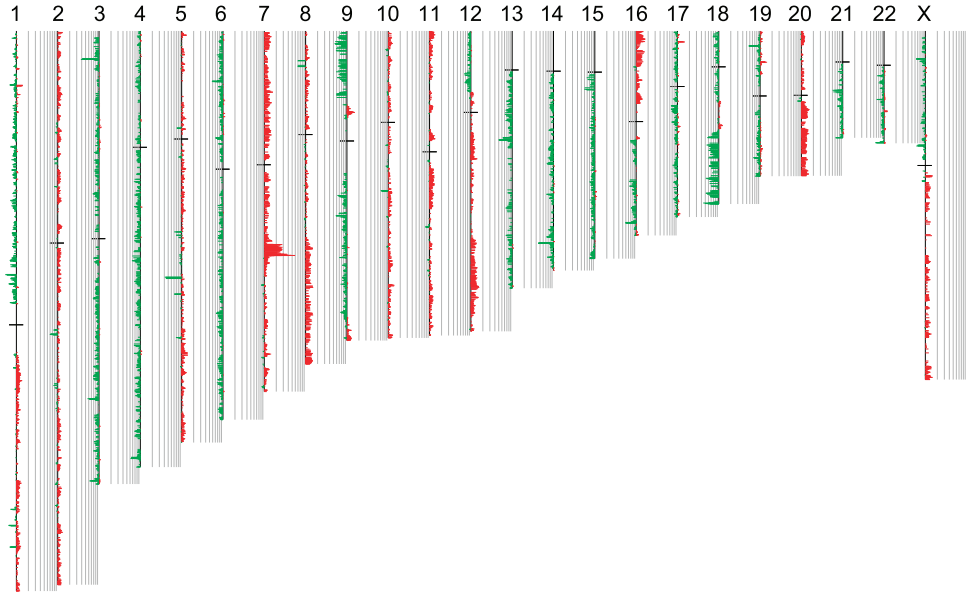

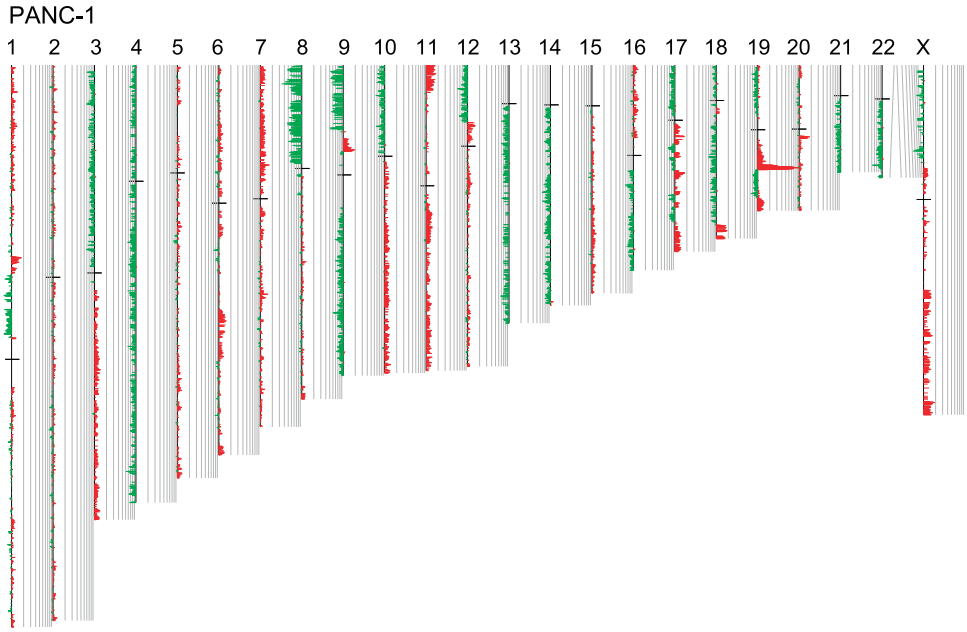
PANC-1
1 2 3 4 5 6 7 8 9 10 11 12 13 14 15 16 17 18 19 20 21 22 X

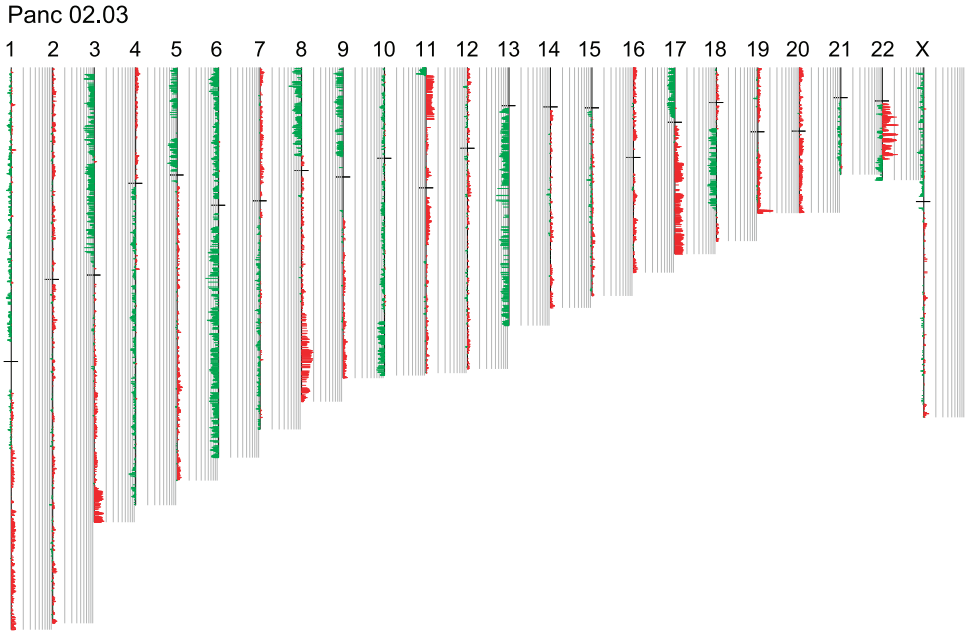
Panc 02.03
1 2 3 4 5 6 7 8 9 10 11 12 13 14 15 16 17 18 19 20 21 22 X

Panc 02.13

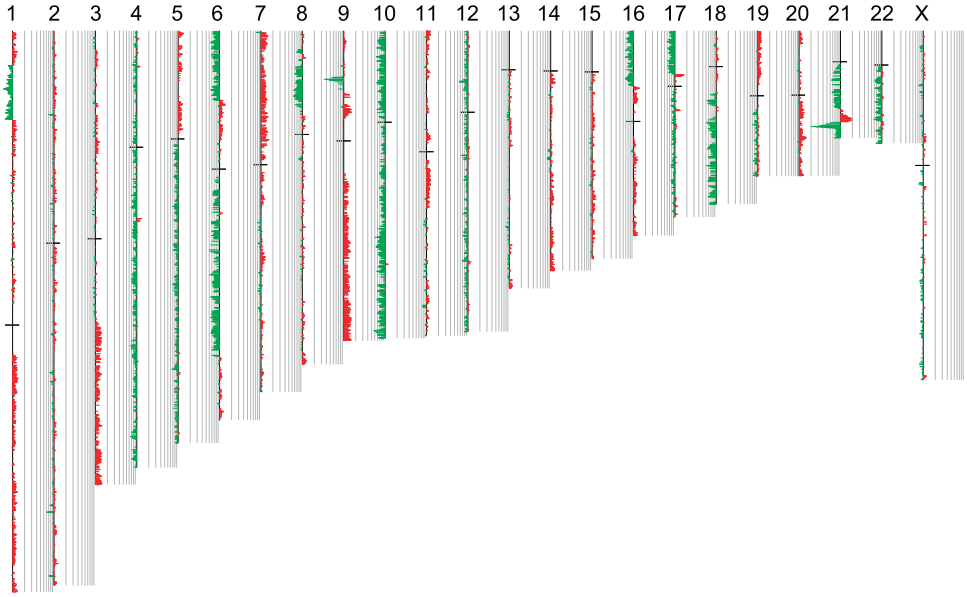

Panc 03.27

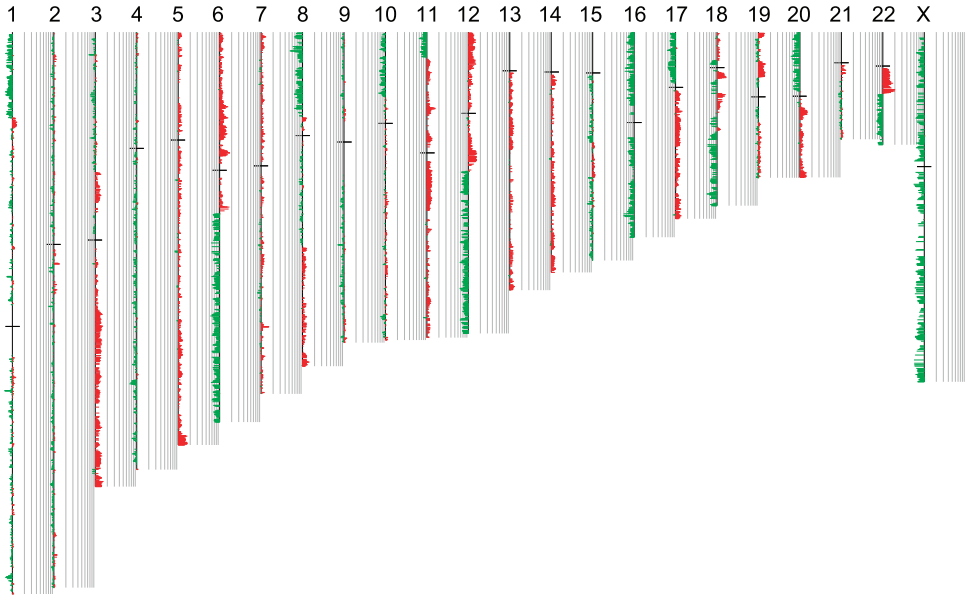

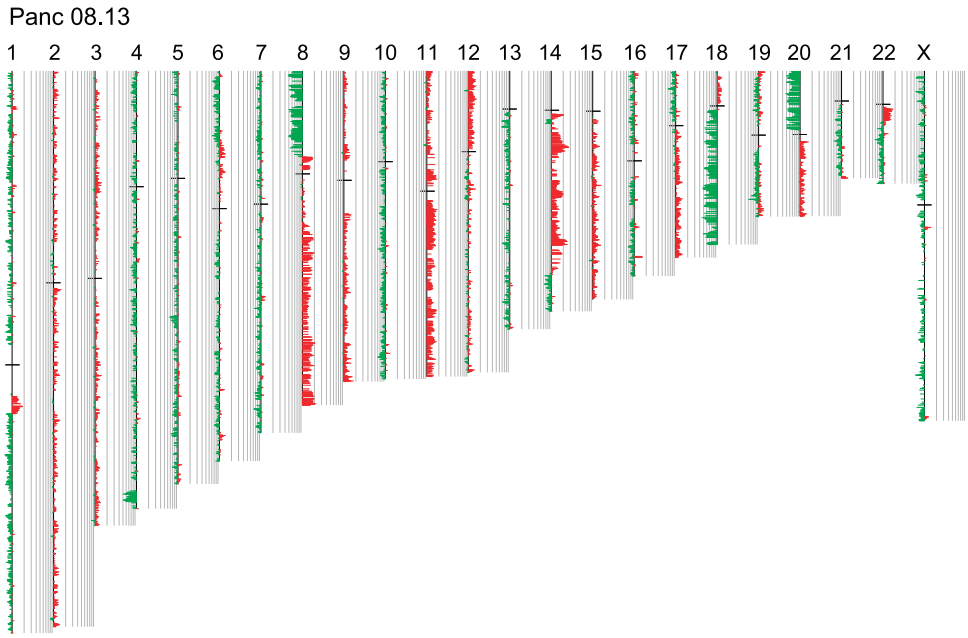
Panc 08.13
1 2 3 4 5 6 7 8 9 10 11 12 13 14 15 16 17 18 19 20 21 22 X

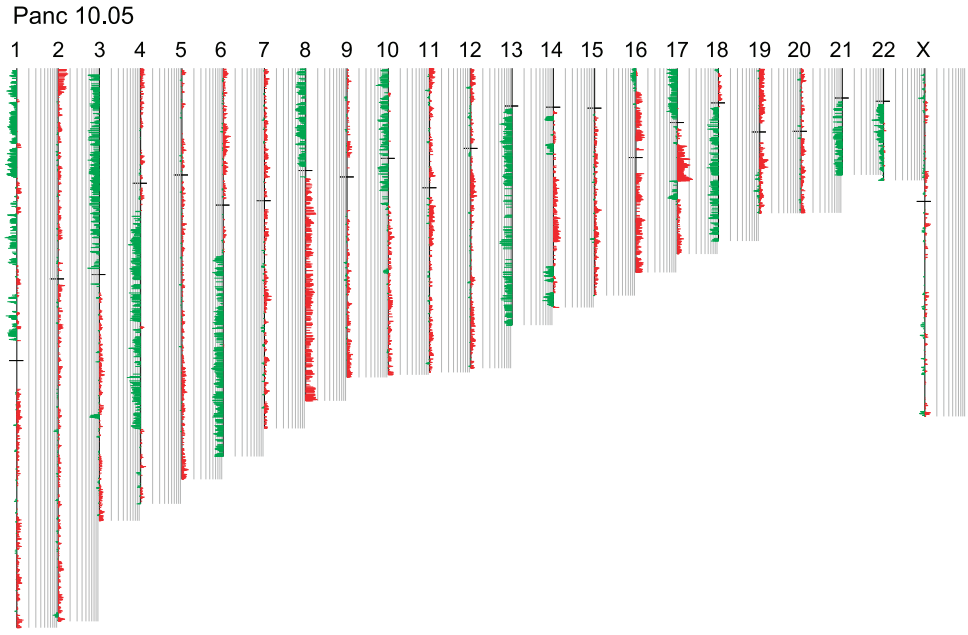
Panc 10.05
1 2 3 4 5 6 7 8 9 10 11 12 13 14 15 16 17 18 19 20 21 22 X

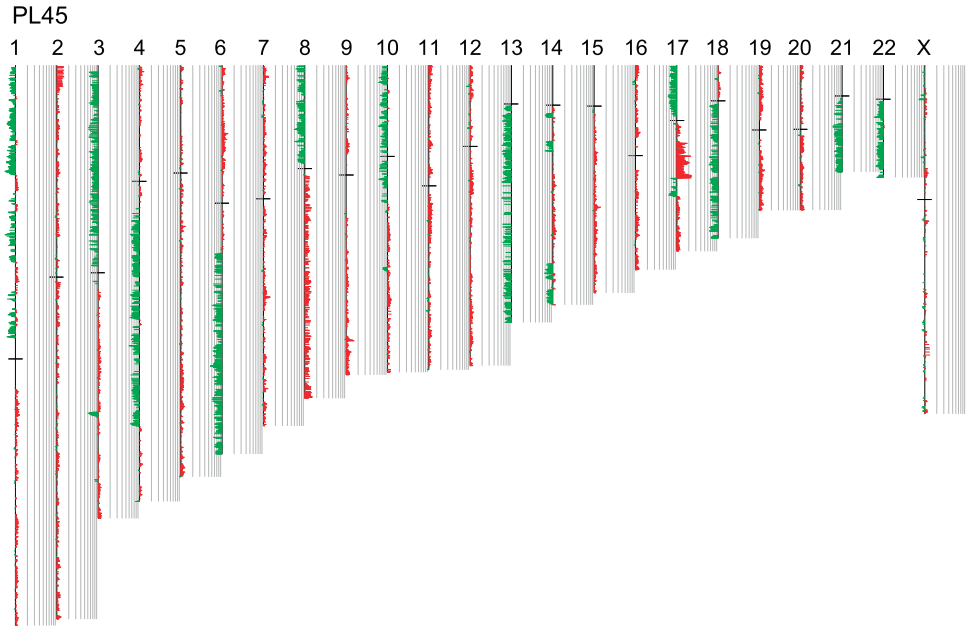
PL45
1 2 3 4 5 6 7 8 9 10 11 12 13 14 15 16 17 18 19 20 21 22 X

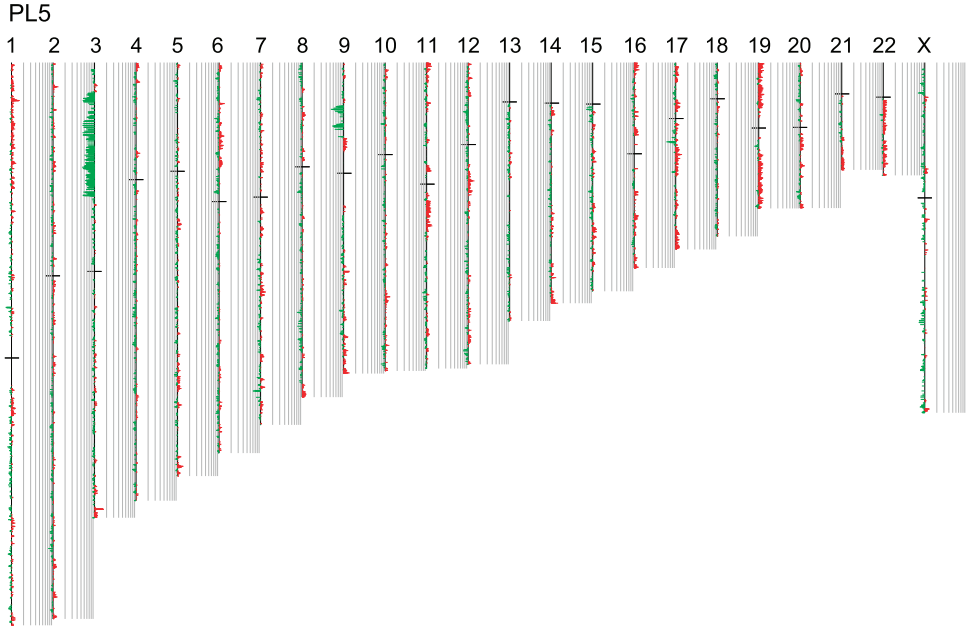
PL5
1 2 3 4 5 6 7 8 9 10 11 12 13 14 15 16 17 18 19 20 21 22 X

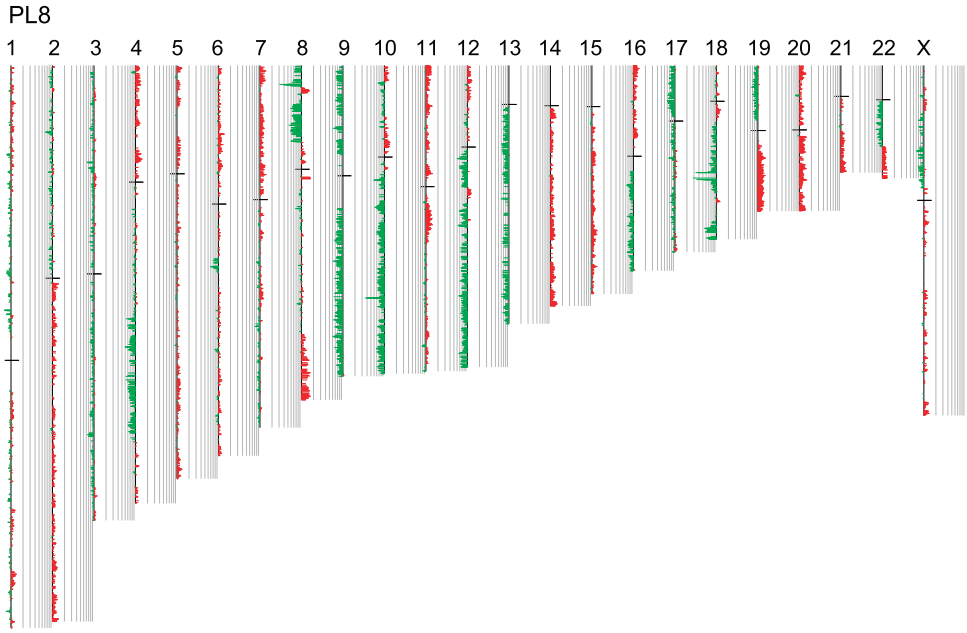
PL8
1 2 3 4 5 6 7 8 9 10 11 12 13 14 15 16 17 18 19 20 21 22 X

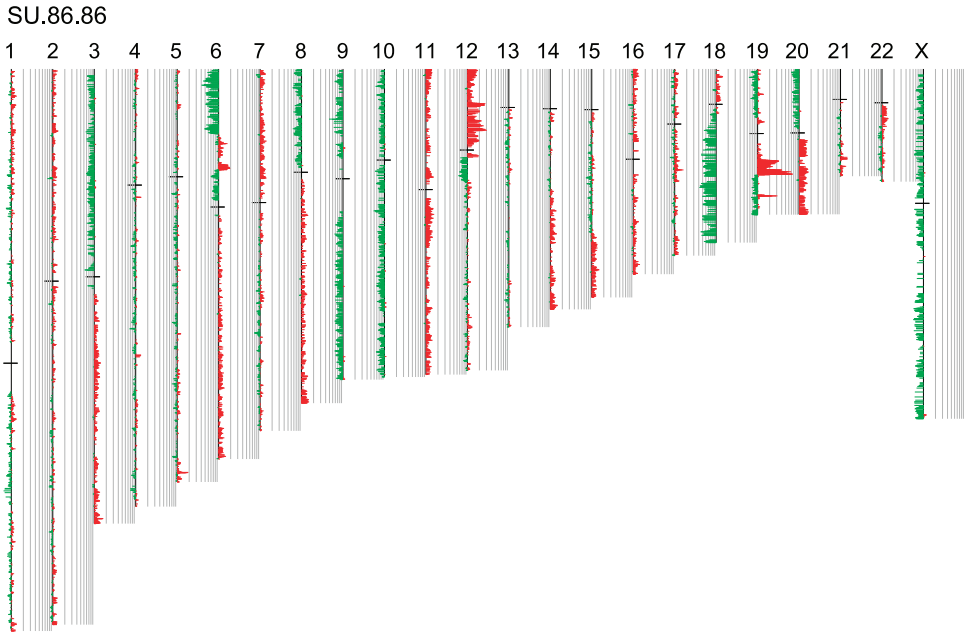
SU.86.86
1 2 3 4 5 6 7 8 9 10 11 12 13 14 15 16 17 18 19 20 21 22 X

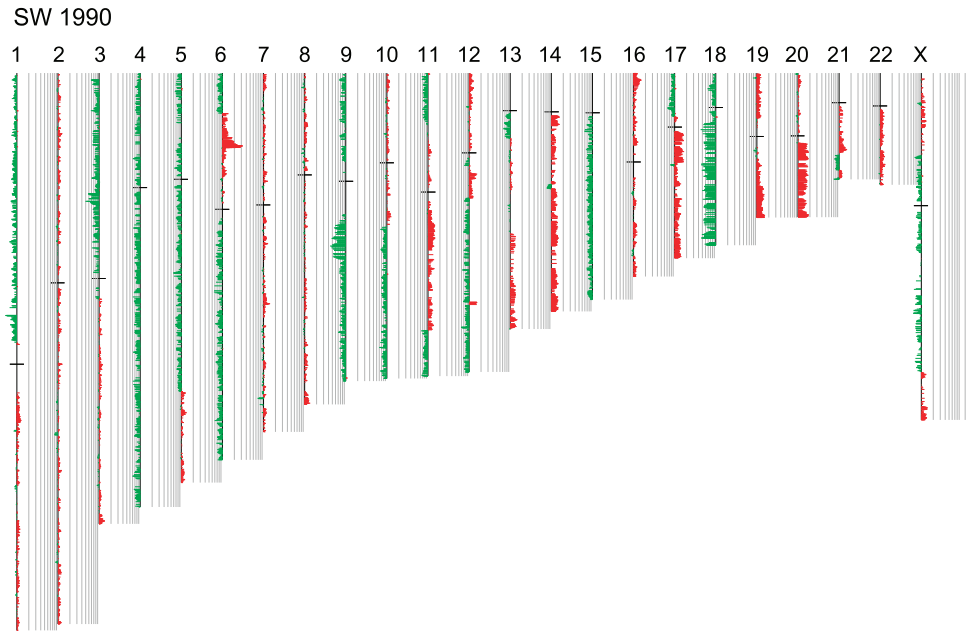
SW 1990
1 2 3 4 5 6 7 8 9 10 11 12 13 14 15 16 17 18 19 20 21 22 X